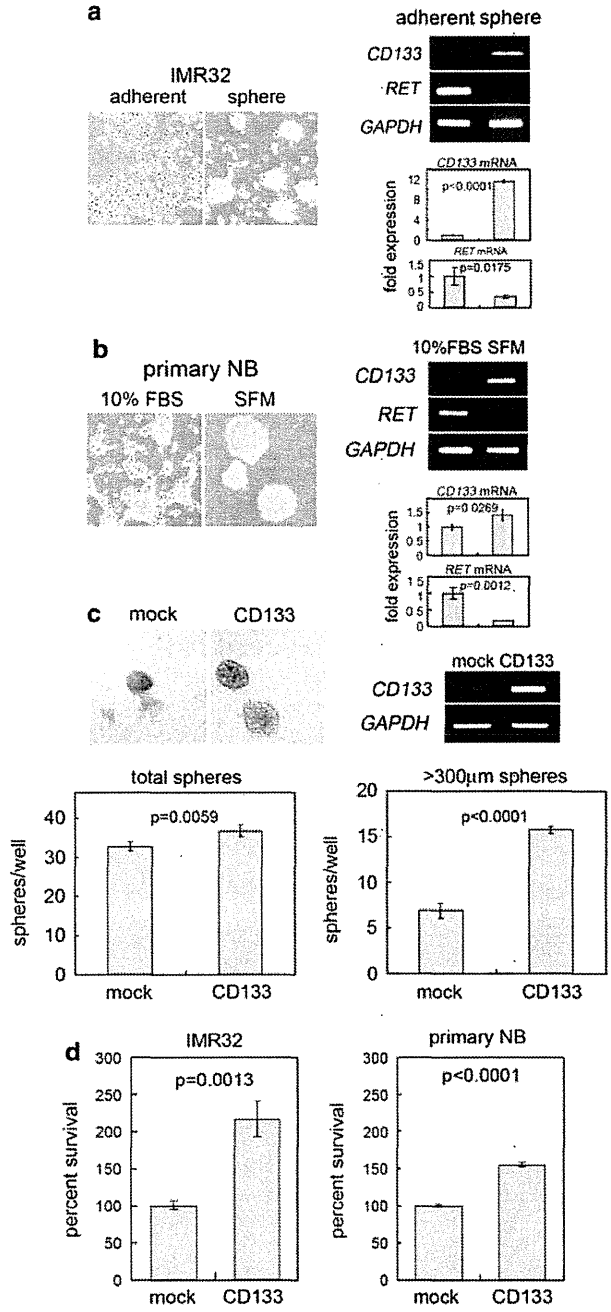

Figure 5 CD133 enhances cellular survival of NB cells in neurospheres. IMR32 cells (**a**) and primary NB cells (**b**) were cultured in 10% fetal bovine serum containing medium (adherent) or SFM (sphere) for a week. Semi-quantitative RT–PCR and qPCR analyses were performed with adherent or sphere cell RNAs using specific primers for *CD133* and *RET*. *GAPDH* was used as a loading control. Primary NB cell results are representative of three tumor samples. (**c**) IMR32 cells were stably infected with mock or CD133-expressing lentivirus. The expression levels of *CD133* and *GAPDH* were determined by semi-quantitative RT–PCR. Cells were cultured in 96-well culture plates with SFM. After 5 weeks, spheres were measured and counted under a microscope with an eyepiece micrometer. (**d**) Enzymatically dissociated IMR32- or primary NB-sphere cells were stained with trypan blue and counted to determine the number of viable cells.

the upregulation of CD133 (1.4-fold induction) and downregulation of RET receptors (5.9-fold reduction) were found in SFM medium, but not in the medium with 10% fetal bovine serum (Figure 5b). Next, we introduced CD133 into IMR32 cells by lentivirus infection, and after 5-week culture in SFM, we found that CD133-expressing cells formed many more large spheres than mock cells (Figure 5c). Moreover, CD133-expressing spheres made from IMR32 and primary NB cells contained many more living cells than the mock control (Figure 5d), suggesting that CD133 promotes NB cell survival in tumor-sphere formation.

Discussion

Increasing evidence highlights the function of CD133 as a marker of CSCs in various human tumors; however, its function in tumorigenesis remains to be elucidated by molecular biology experiments. In this study, CD133-knockdown experiments indicated that CD133 represses differentiation in NB cells; CD133 was clearly decreased by differentiation-inducing stimulation, for example ATRA and TPA treatments. Brodeur *et al.* (2000) indicated that neurotrophic factors and their receptors have a significant function in NB behavior and the potential to send intracellular signals into the nucleus to produce neuronal differentiation in the normal sympathetic nerve system. Among the NB cell differentiation-related neurotrophic receptors, *RET* transcription was regulated by CD133 in NB cell lines. The expression of CD133 effectively inhibited NB cell differentiation (neurite extension and differentiation markers). Furthermore, RET expression partly rescued the CD133-related inhibition of differentiation. These findings suggest that CD133-mediated RET suppression has a considerable function in NB cell differentiation. Regarding the function of RET in NB differentiation, Peterson and Bogenmann (2004) suggested that RET receptor activation inhibits cell cycle progression and enhances responsiveness to NGF; thus, NB cell differentiation requires the collaboration of functional RET and TrkA signal pathways; they also reported that GDNF treatment induced *RET* transcription in NB cells. Intriguingly, our results indicate that CD133 expression effectively suppressed *RET* mRNA in NB cells and CD133 knockdown induced NB cell differentiation, suggesting that suppression of CD133 by small-interference RNA administration will increase *RET* transcription in CD133-expressing NB tumors and may be useful in differentiation induction therapy for resistant- and relapsed-NB tumors. In addition, transcriptional suppression of *CD133* could be useful to induce differentiation in NB cells; however, the exact mechanism of transcriptional regulation of CD133 has not been clarified. Although seven CD133 mRNA isoforms controlled by five alternative promoters were reported previously (Shmelkov *et al.*, 2004), the promoter activities of these isoforms were studied only by pGL3-enhancer vector, suggesting the existence of other *cis*-elements in the CD133 locus.

Several studies have been reported to elucidate the molecular mechanism and signaling pathways that regulate the behavior of CD133-expressing cancer cells. Nikolova *et al.* (2007) reported that WNT-conditional media had effects on the proliferation and differentiation of cord blood-derived CD133-positive cells, and Fan *et al.* (2006) showed that Notch signal inhibition by GSI-18 reduced the CD133-positive fraction in brain tumor cells. Regarding the analysis of the intracellular signaling pathway related to the CD133 function, one report suggested the significance of the Akt/PKB pathway in the expression of survival proteins, phosphor-Bad and Bcl-2 in CD133-positive hepatocellular carcinoma cell survival (Ma *et al.*, 2007). In our study, CD133-knockdown experiments indicated that CD133-related RET repression and NB cell differentiation were caused by signal pathway activation, for example p38MAPK and PI3K/Akt pathways. To support this observation, treatment with kinase inhibitors showed a correlation between neurite elongation and RET induction in NB cells, and that differentiation marker protein induction was mainly dependent on the p38MAPK pathway. These findings suggest that CD133 prevents NB cell differentiation via signal transduction pathways. To the best of our knowledge, this is the first report of CD133-related signal pathway modification resulting in cell differentiation. As CD133 is a membranous protein on stem cells and cancer stem cells, it is possible that CD133 affects membranous receptor functions and the downstream signal pathways. In addition, Boivin *et al.* (2009) reported the phosphorylation of CD133-cytoplasmic tyrosine-828 and tyrosine-852 by Src and Fyn tyrosine kinases. Site-directed mutagenesis of these tyrosine residues in CD133 will provide important information for CD133 functions in our experimental system using NB cells.

Materials and methods

Cell culture and reagents

Human NB cell lines were obtained from official cell banks (RIKEN Cell Bank, Tsukuba, Japan and ATCC, Manassas, VA, USA) and cultured in high-glucose DMEM (Sigma-Aldrich, St Louis, MO, USA) or RPMI1640 (Wako, Osaka, Japan) supplemented with 10% heat-inactivated fetal bovine serum (Invitrogen, Carlsbad, CA, USA) and 50 μg/ml penicillin/streptomycin (Sigma-Aldrich) in an incubator with humidified air at 37 °C with 5% CO_2. NB cell lines subjected to molecular biology and biochemistry experiments were MYCN single-copy SH-SY5Y cells and MYCN-amplified TGW, SK-N-DZ and IMR32 cells. GDNF was obtained from Invitrogen. ATRA was from Sigma-Aldrich. Phorbol-12-myristate-13-acetate (TPA) was from Nacalai Tesque (Kyoto, Japan). LY294002 was from Cell Signaling Technology (Beverly, MA, USA). PD98059 and SB203580 were from Calbiochem (San Diego, CA, USA).

Fluorescence-activated cell sorting analysis

NB cell lines growing in the log phase were enzymatically removed from 10 cm diameter culture dishes, washed with cold PBS and treated with biotinylated AC133 (CD133/1) monoclonal antibodies (Miltenyi Biotec, Auburn, CA, USA) or control IgG2A (eBioscience, San Diego, CA, USA) for 15 min at 4 °C. The primary antibody was removed, and then the cells were washed twice with ice-cold PBS containing 0.1% BSA, and a 1:200 dilution of phycoerythrin-labeled streptavidin (eBioscience) added for 15 min at 4 °C. After washing, flow cytometry was performed using a fluorescence-activated cell sorting Caliber (BD, San Jose, CA, USA).

Knockdown of CD133

For RNAi experiments, predesigned, double-stranded SMART-pool small-interference RNA targeting human *CD133* (*prominin-1*) was purchased from Dharmacon (Lafayette, CO, USA) and Silencer Negative Control small-interference RNA #1 was purchased from Ambion (Austin, TX, USA).

Lentivirus-mediated gene transduction and knockdown

The packaging cell line HEK 293T (4×10^6) was plated and transfected the following day. Then, 1.5 μg transducing vectors containing the gene [pHR-SIN-CMV-G-DL1 or CSII-CMV-MCS-IRES2-Bsd vector (RIKEN Bioresource Center, Ibaraki, Japan)] or shRNA [pLKO.1 (Sigma-Aldrich)] and 2.0 μg packaging vectors (Sigma-Aldrich) were co-transfected with Fugene 6 transfection reagent (Roche Applied Science, Indianapolis, IN, USA) according to the manufacturer's protocols. The medium was changed the following day, and cells were cultured for another 24 h. Conditioned medium was collected and cleared of debris by filtering through a 0.45 μm filter (Millipore, Bedford, MA, USA). Then, 1×10^5 NB cells were seeded in each well of a six-well plate, and transduced by lentiviral-conditioned media. Transduced cells were analyzed by western blotting and RT–PCR.

Cloning of human CD133 cDNA

The human *CD133* cDNA (RefSeq NM_006017) was cloned from human colon cancer cell line Caco-2 mRNA by RT–PCR using specific primer sets described in Supplementary Table 1S. *CD133* cDNA fragment was sub-cloned into a lentiviral-based vector (pHR-SIN-CSGW) (Hasegawa *et al.*, 2006).

Western blot analysis

The cells were lysed in buffer containing 5 mM EDTA, 2 mM Tris–HCl (pH 7.5), 10 mM β-glycerophosphate, 5 μg/ml aprotinin, 2 mM phenylmethylsulfonyl fluoride, 1 mM Na_3VO_4, a protease inhibitor cocktail (Nacalai Tesque) and 1% SDS. Western blot analysis was performed as reported previously (Kurata *et al.*, 2008). For CD133 detection, we used AC133 monoclonal antibody. Anti-RET (Santa Cruz Biotechnology, Santa Cruz, CA, USA), anti-phospho- and total Akt, p38, ERK (Cell Signaling Technology) and anti-tubulin antibody from Lab Vision (Fremont, CA, USA) were also used.

Semi-quantitative RT–PCR

Semi-quantitative RT–PCR analysis was as described previously (Kurata *et al.*, 2008). Total cellular RNA for preparing RT–PCR templates was extracted using ISOGEN (Nippon Gene KK, Tokyo, Japan). The cDNA was synthesized from 1 μg total RNA and then subjected to PCR. Primer sequences are described in Supplementary Table 1S. RT–PCR results are representative of at least three independent experiments.

qPCR analysis

The qPCR analysis was performed as described previously (Ochiai *et al.*, 2010). The primers for qPCR were designed and synthesized to produce 50–150 bp products. The primer sequence is listed in Supplementary Table 1S. The results were representative of at least three independent experiments.

Cell proliferation and soft agar assay
Cells were seeded into 96-well plates (750 per well) in culture medium containing 10% fetal bovine serum. Every 24 h, cell viability was determined by water-soluble tetrazolium salt (WST-8) assay using Counting kit-8 (Dojindo, Kumamoto, Japan) according to the manufacturer's protocol. For soft agar assay, 2×10^3 cells of stable infectants TGW or SH-SY5Y cells were seeded in soft agar as described previously (Aoyama *et al.*, 2005). Viable colonies were stained with 0.05 mg/ml MTT.

Tumor formation in nude mice
For tumor formation, 6-week-old female athymic BALB/c AJcl *nu/nu* mice (CLEA Japan, Shizuoka, Japan) were injected into the femur with 1×10^7 TGW cells as described previously (Aoyama *et al.*, 2005). The handling of animals was in accordance with the guidelines of Chiba Cancer Center Research Institute.

Patients and tumor specimens
The 12 tumor specimens used in this study were kindly provided by various institutions and hospitals in Japan. Informed consent was obtained at each institution or hospital. All tumors were diagnosed clinically as well as pathologically as NB and staged according to the International NB Staging System criteria. The patients were treated by standard chemotherapy protocols as described previously (Kaneko *et al.*, 2002; Iehara *et al.*, 2006). *MYCN* copy number, *TrkA* mRNA expression levels and DNA index were measured as reported previously (Ohira *et al.*, 2003). This study was approved by the Institutional Review Board of Chiba Cancer Center.

Subcloning of human RET (RET9)
Human *RET9* (Crowder *et al.*, 2004) full-length cDNA was a kind gift from Dr Hideki Enomoto (RIKEN Center for Developmental Biology, Hyogo, Japan). *RET9* cDNA fragment (3.4 kb) was sub-cloned into the *Not*I site of CSII-CMV-MCS-IRES2-Bsd vector, which had been altered to accept the *Xba*I and *Hin*dIII ends.

Cloning of human RET promoter
Human *RET* promoter 1.5 kb (−919 to +550, position +1 is the transcription start site determined in a previous report (Itoh *et al.*, 1992)) was amplified from human genomic DNA using Platinum *Pfx* polymerase (Invitrogen) with primers (described in Supplementary Table 1S) by PCR amplification and sub-cloned into pGEM-T easy vector (Promega, Southampton, UK). The *RET* 5′-flanking sequence from −453 to +227 was sub-cloned into the *Eco*RV site of pGL4.17 reporter vector (Promega).

Sphere culture of NB cells
The preparation of primary NB cells from stage 4 patients' bone marrow was described previously (Nakanishi *et al.*, 2007). Dissociated primary NB cells or IMR32 cells were cultured in SFM (DMEM-F12, 1:1 (Wako), 50 μg/ml penicillin/streptomycin, 2% B27 supplement (Invitrogen), 20 ng/ml epidermal growth factor (Sigma-Aldrich) and 20 ng/ml fibroblast growth factor basic (Invitrogen)). Half of the medium was replaced with fresh culture medium every 7 days. IMR32 cells and primary NB cells were seeded in 96-well (400 per well) or six-well (1×10^5 per well) and six-well (1.7×10^5 per well) plates, respectively. Spheres were counted and measured under a microscope with an eyepiece micrometer. Five-week cultured IMR32 or 2-month cultured primary NB spheres were dissociated by Accumax (Innovative Cell Technologies, San Diego, CA, USA) according to the manufacturer's protocol. Living cells were counted based on morphological criteria and trypan blue staining.

Conflict of interest

The authors declare no conflict of interest.

Acknowledgements

We thank K Sakurai and S Matsushita for technical assistance, Dr Hiroyuki Miyoshi (BioResource Center, RIKEN) for the gift of CSII-CMV-MCS-IRES2-Bsd plasmid and Daniel Mrozek, Medical English Service, for editorial assistance. This work was supported in part by a grant-in-aid from JSPS for Young Scientists (B) (number: 19790274), a grant-in-aid from the Ministry of Health, Labor, and Welfare for Third Term Comprehensive Control Research for Cancer, a grant-in-aid for Cancer Research (20–13) from the Ministry of Health, Labor, and Welfare of Japan and a grant-in-aid from the Ministry of Education, Culture, Sports, Science and Technology, Japan (number: 21591377).

References

Aoyama M, Ozaki T, Inuzuka H, Tomotsune D, Hirato J, Okamoto Y *et al.* (2005). LMO3 interacts with neuronal transcription factor, HEN2, and acts as an oncogene in neuroblastoma. *Cancer Res* **65**: 4587–4597.

Boivin D, Labbé D, Fontaine N, Lamy S, Beaulieu E, Gingras D *et al.* (2009). The stem cell marker CD133 (prominin-1) is phosphorylated on cytoplasmic tyrosine-828 and tyrosine-852 by Src and Fyn tyrosine kinases. *Biochemistry* **48**: 3998–4007.

Brodeur GM, Sawada T, Tsuchida Y, Voute PA (eds) (2000). *Neuroblastoma.* Elsevier Science: Amsterdam.

Collins AT, Berry PA, Hyde C, Stower MJ, Maitland NJ. (2005). Prospective identification of tumorigenic prostate cancer stem cells. *Cancer Res* **65**: 10946–10951.

Corbeil D, Roper K, Hellwig A, Tavian M, Miraglia S, Watt SM *et al.* (2000). The human AC133 hematopoietic stem cell antigen is also expressed in epithelial cells and targeted to plasma membrane protrusions. *J Biol Chem* **275**: 5512–5520.

Corbeil D, Fargeas CA, Huttner WB. (2001). Rat prominin, like its mouse and human orthologues, is a pentaspan membrane glycoprotein. *Biochem Biophys Res Commun* **285**: 939–944.

Crowder RJ, Enomoto H, Yang M, Johnson Jr EM, Milbrandt J. (2004). Dok-6, a Novel p62 Dok family member, promotes Ret-mediated neurite outgrowth. *J Biol Chem* **279**: 42072–42081.

D'Alessio A, De Vita G, Cali G, Nitsch L, Fusco A, Vecchio G *et al.* (1995). Expression of the RET oncogene induces differentiation of SK-N-BE neuroblastoma cells. *Cell Growth Differ* **6**: 1387–1394.

Enomoto H, Crawford PA, Gorodinsky A, Heuckeroth RO, Johnson Jr EM, Milbrandt J. (2001). RET signaling is essential for migration, axonal growth and axon guidance of developing sympathetic neurons. *Development* **128**: 3963–3974.

Enomoto H, Heuckeroth RO, Golden JP, Johnson EM, Milbrandt J. (2000). Development of cranial parasympathetic ganglia

requires sequential actions of GDNF and neurturin. *Development* **127**: 4877–4889.
Fan X, Matsui W, Khaki L, Stearns D, Chun J, Li YM *et al.* (2006). Notch pathway inhibition depletes stem-like cells and blocks engraftment in embryonal brain tumors. *Cancer Res* **66**: 7445–7452.
Hansford LM, McKee AE, Zhang L, George RE, Gerstle JT, Thorner PS *et al.* (2007). Neuroblastoma cells isolated from bone marrow metastases contain a naturally enriched tumor-initiating cell. *Cancer Res* **67**: 11234–11243.
Hasegawa K, Nakamura T, Harvey M, Ikeda Y, Oberg A, Figini M *et al.* (2006). The use of a tropism-modified measles virus in folate receptor-targeted virotherapy of ovarian cancer. *Clin Cancer Res* **12**: 6170–6178.
Itoh F, Ishizaka Y, Tahira T, Yamamoto M, Miya A, Imai K *et al.* (1992). Identification and analysis of the *ret* proto-oncogene promoter region in neuroblastoma cell lines and medullary thyroid carcinomas from MEN2A patients. *Oncogene* **7**: 1201–1206.
Iehara T, Hosoi H, Akazawa K, Matsumoto Y, Yamamoto K, Suita S *et al.* (2006). MYCN gene amplification is a powerful prognostic factor even in infantile neuroblastoma detected by mass screening. *Br J Cancer* **94**: 1510–1515.
Jordan CT, Guzman ML, Noble M. (2006). Cancer stem cells. *N Engl J Med* **355**: 1253–1261.
Kaplan D, Matsumoto K, Lucarelli E, Thiele CJ. (1993). Induction of TrkB by retinoic acid mediates biologic responsiveness to BDNF and differentiation of human neuroblastoma cells. Eukaryotic Signal Transduction Group. *Neuron* **11**: 321–331.
Kaneko M, Tsuchida Y, Mugishima H, Ohnuma N, Yamamoto K, Kawa K *et al.* (2002). Intensified chemotherapy increases the survival rates in patients with stage 4 neuroblastoma with MYCN amplification. *J Pediatr Hematol Oncol* **24**: 613–621.
Klein R. (1994). Role of neurotrophins in mouse neuronal development. *FASEB J* **8**: 738–744.
Kurata K, Yanagisawa R, Ohira M, Kitagawa M, Nakagawara A, Kamijo T. (2008). Stress via p53 pathway causes apoptosis by mitochondrial Noxa upregulation in doxorubicin-treated neuroblastoma cells. *Oncogene* **27**: 741–754.
Ma S, Lee TK, Zheng BJ, Chan KW, Guan XY. (2007). CD133+ HCC cancer stem cells confer chemoresistance by preferential expression of the Akt/PKB survival pathway. *Oncogene* **27**: 1749–1758.
Maris JM, Hogarty MD, Bagatell R, Cohn SL. (2007). Neuroblastoma. *Lancet* **369**: 2106–2120.
Maw MA, Corbeil D, Koch J, Hellwig A, Wilson-Wheeler JC, Bridges RJ *et al.* (2000). A frameshift mutation in prominin (mouse)-like 1 causes human retinal degeneration. *Hum Mol Genet* **9**: 27–34.
Miki J, Furusato B, Li H, Gu Y, Takahashi H, Egawa S *et al.* (2007). Identification of putative stem cell markers, CD133 and CXCR4, in hTERT-immortalized primary nonmalignant and malignant tumor derived human prostate epithelial cell lines and in prostate cancer specimens. *Cancer Res* **67**: 3153–3161.
Monzani E, Facchetti F, Galmozzi E, Corsini E, Benetti A, Cavazzin C *et al.* (2007). Melanoma contains CD133 and ABCG2 positive cells with enhanced tumourigenic potential. *Eur J Cancer* **43**: 935–946.
Myers SM, Eng C, Ponder BA, Mulligan LM. (1995). Characterization of RET proto-oncogene 3′ splicing variants and polyadenylation sites: a novel C-terminus for RET. *Oncogene* **11**: 2039–2045.
Nakanishi H, Ozaki T, Nakamura Y, Hashizume K, Iwanaka T, Nakagawara A. (2007). Purification of human primary neuroblastomas by magnetic beads and their *in vitro* culture. *Oncol Rep* **17**: 1315–1320.
Nikolova T, Wu M, Brumbarov K, Alt R, Opitz H, Boheler KR *et al.* (2007). WNT-conditioned media differentially affect the proliferation and differentiation of cord blood-derived CD133+ cells *in vitro*. *Differentiation* **75**: 100–111.
O'Brien CA, Pollett A, Gallinger S, Dick JE. (2007). A human colon cancer cell capable of initiating tumour growth in immunodeficient mice. *Nature* **445**: 106–110.
Ochiai H, Takenobu H, Nakagawa A, Yamaguchi Y, Kimura M, Ohira M *et al.* (2010). Bmi1 is a MYCN target gene that regulates tumorigenesis through repression of *KIF1Bβ* and *TSLC1* in neuroblastoma. *Oncogene* **29**: 2681–2690.
Ohira M, Morohashi A, Inuzuka H, Shishikura T, Kawamoto T, Kageyama H *et al.* (2003). Expression profiling and characterization of 4200 genes cloned from primary neuroblastomas: identification of 305 genes differentially expressed between favorable and unfavorable subsets. *Oncogene* **22**: 5525–5536.
Olempska M, Eisenach PA, Ammerpohl O, Ungefroren H, Fandrich F, Kalthoff H. (2007). Detection of tumor stem cell markers in pancreatic carcinoma cell lines. *Hepatobiliary Pancreat Dis Int* **6**: 92–97.
Peterson S, Bogenmann E. (2004). The RET and TRKA pathways collaborate to regulate neuroblastoma differentiation. *Oncogene* **23**: 213–225.
Reya T, Morrison SJ, Clarke MF, Weissman IL. (2001). Stem cells, cancer, and cancer stem cells. *Nature* **414**: 105–111.
Ricci-Vitiani L, Lombardi DG, Pilozzi E, Biffoni M, Todaro M, Peschle C *et al.* (2007). Identification and expansion of human colon-cancer initiating cells. *Nature* **445**: 111–115.
Shmelkov SV, Jun L, St Clair R, McGarrigle D, Derderian CA, Usenko JK *et al.* (2004). Alternative promoters regulate transcription of the gene that encodes stem cell surface protein AC133. *Blood* **103**: 2055–2061.
Singh SK, Hawkins C, Clarke ID, Squire JA, Bayani J, Hide T *et al.* (2004). Identification of human brain tumour initiating cells. *Nature* **432**: 396–401.
Walton JD, Kattan DR, Thomas SK, Spengler BA, Guo HF, Biedler JL *et al.* (2004). Characteristics of stem cells from human neuroblastoma cell lines and in tumors. *Neoplasia* **6**: 838–845.
Weinberg RA (ed) (2006). *The Biology of Cancer*. Garland Science: New York.
Yin AH, Miraglia S, Zanjani ED, Almeida-Porada G, Ogawa M, Leary AG *et al.* (1997). AC133, a novel marker for human hematopoietic stem and progenitor cells. *Blood* **90**: 5002–5012.
Yin S, Li J, Hu C, Chen X, Yao M, Yan M *et al.* (2007). CD133 positive hepatocellular carcinoma cells possess high capacity for tumorigenicity. *Int J Cancer* **120**: 1444–1450.
Zacchigna S, Oh H, Wilsch-Bräuninger M, Missol-Kolka E, Jászai J, Jansen S *et al.* (2009). Loss of the cholesterol-binding protein prominin-1/CD133 causes disk dysmorphogenesis and photoreceptor degeneration. *J Neurosci* **29**: 2297–2308.

Supplementary Information accompanies the paper on the Oncogene website (http://www.nature.com/onc)

SCIENTIFIC REPORTS

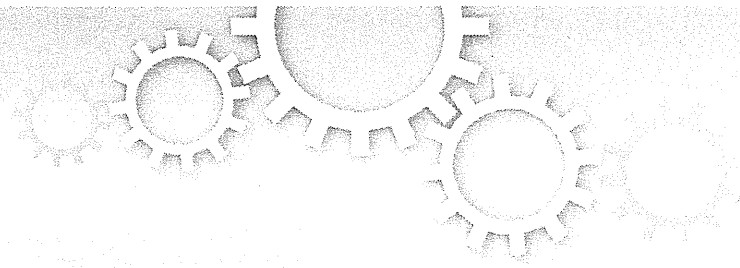

SUBJECT AREAS:
CANCER
CANCER MODELS
CELL DEATH
ONCOGENESIS

Received
22 February 2011

Accepted
25 March 2011

Published
14 June 2011

Correspondence and requests for materials should be addressed to A.T. (atsushit@sentan.med.kyushu-u.ac.jp)

* deceased

A novel potent tumour promoter aberrantly overexpressed in most human cancers

Atsushi Takahashi[1,2,4], Hisashi Tokita[3]*, Kenzo Takahashi[5], Tomoharu Takeoka[4], Kosho Murayama[1], Daihachiro Tomotsune[2], Miki Ohira[2], Akihiro Iwamatsu[6], Kazuaki Ohara[7], Kazufumi Yazaki[7], Tadayuki Koda[8], Akira Nakagawara[2] & Kenzaburo Tani[1]

[1]Division of Molecular and Clinical Genetics, Department of Molecular Genetics, Medical Institute of Bioregulation, Kyushu University, Fukuoka 812-8582, Japan, [2]Division of Biochemistry and [3]Division of Animal Science, Chiba Cancer Center Research Institute, Chiba 260-8717, Japan, [4]Department of Hematology and Oncology and [5]Department of Dermatology, Graduate School of Medicine, Kyoto University, Kyoto 606-8507, Japan, [6]Protein Research Network, Inc., Yokohama, Kanagawa 236-0004, Japan, [7]Laboratory of Plant Gene Expression, Research Institute for Sustainable Humanosphere, Kyoto University, Uji 611-0011, Japan, [8]Hisamitsu Pharmaceutical Co., Inc., Tokyo 100-6221, Japan.

The complexity and heterogeneity of tumours have hindered efforts to identify commonalities among different cancers. Furthermore, because we have limited information on the prevalence and nature of ubiquitous molecular events that occur in neoplasms, it is unfeasible to implement molecular-targeted cancer screening and prevention. Here, we found that the FEAT protein is overexpressed in most human cancers, but weakly expressed in normal tissues including the testis, brain, and liver. Transgenic mice that ectopically expressed FEAT in the thymus, spleen, liver, and lung spontaneously developed invasive malignant lymphoma (48%, 19/40) and lung-metastasizing liver cancer (hepatocellular carcinoma) (35%, 14/40) that models human hepatocarcinogenesis, indicating the FEAT protein potently drives tumorigenesis *in vivo*. Gene expression profiling suggested that FEAT drives receptor tyrosine kinase and hedgehog signalling pathways. These findings demonstrate that integrated efforts to identify FEAT-like ubiquitous oncoproteins are useful and may provide promising approaches for cost-effective cancer screening and prevention.

Although our understanding of the molecular mechanisms of carcinogenesis has greatly improved, this knowledge has not lead to the identification and development of effective tools for cancer screening and prevention [1]. Approximately 30–40% of all cancer deaths are preventable, and this estimation is based on indirect measures that do not interfere with carcinogenesis, such as dietary modifications, lifestyle changes, minimizing carcinogen exposure, and vaccination against oncogenic viruses [1]. More advanced chemoprevention measures such as tamoxifen, raloxifene, finasteride, and celecoxib [1] and the eradication of *Helicobacter pylori* are only available to high-risk groups for particular cancers.

In order to reach the long-term goal of establishing molecular-targeted cancer screening and prevention, it is important that we explore, characterize, and catalogue a distinct subclass of cancer genes [2] that are involved in diverse cancers. However, the systematic approaches that have been used to identify cancer genes, such as sequencing protein-coding exons [3–9], whole genome sequencing [10,11], and paired-end sequencing to comprehensively identify somatic rearrangements [12], have only further emphasized the marked heterogeneity and complexity of human neoplasms and have not successfully identified commonalities among cancers. Driver mutations that contribute to the development of human cancers [13] are highly variable among different types of cancer and among individual tumours of the same type. Thus, it is still unknown if there are oncogenic molecules that are commonly altered in diverse cancers.

There is accumulating evidence that cancers have heterogeneous combinations of deregulated cancer genes [13,14] and that signalling pathways rather than individual genes are the targets in tumorigenesis [15]. Although some canonical signalling pathways are universally deregulated in cancers, different components of these pathways can be affected in different tumours [3,5–9,15]. The proteins that are commonly overexpressed in cancers are predominantly thought to reflect "peripheral" changes [2,15] that result from neoplastic phenotypes (i.e., augmented metabolic and homeostatic processes such as glycolysis, macromolecular synthesis, and DNA replication) [16,17] and the

resulting "stress phenotype" [18]. Thus, these proteins have not been considered as targets for cancer therapy and prevention. However, this presumption has not been rigorously tested *in vivo* [19].

In the present study, we found that FEAT protein (*f*aint *e*xpression in normal tissues, *a*berrant overexpression in *t*umours) is uniformly overexpressed in a variety of human cancers. Remarkably, FEAT transgenic mice indicated that FEAT potently drives tumorigenesis *in vivo*. Expression microarray analyses suggested that FEAT induces oncogenic pathways. The significance of overexpressed genes in cancer is increasingly recognized as potential leads for a variety of diagnostic and therapeutic approaches [6,7,20]. Additional studies that identify and characterize FEAT-like oncogenic proteins will hopefully advance molecular-targeted cancer screening and prevention.

Results

Biochemical purification of FEAT protein. On analyses of molecules regulating nuclear apoptosis in a cell-free system [21,22], we noticed that the apoptosis-inducing activity was attenuated in the middle of active fractions, concomitant with the appearance of two polypeptides with apparent molecular masses of 74 and 66 kDa (Supplementary Fig. 1). This suggested that apoptosis inhibitors were copurified with apoptosis inducers. Microsequencing revealed that the 74 kDa protein is a rat homologue of human CGI-01 protein [23] that is encoded by *METTL13* (methyltransferase like 13) gene (also known as *KIAA0859*). CGI-01, renamed FEAT, contains two S-adenosylmethionine-binding motifs (SAM-binding motifs) that are characteristic of methyltransferases and related enzymes (see Fig. 1f) [24], and the structure is well conserved across species (Supplementary Fig. 2). Capture compounds mass spectrometry using S-adenosylhomocysteine has detected the *Arabidopsis thaliana* orthologue of FEAT (At2g31740) [25], suggesting that FEAT can bind SAM. We did not detect protein methyltransferase activity, spermidine/spermine synthase activity, or ubiquinone synthase activity (Supplementary Fig. 3) in full-length or truncated FEAT proteins (Supplementary Note). Further

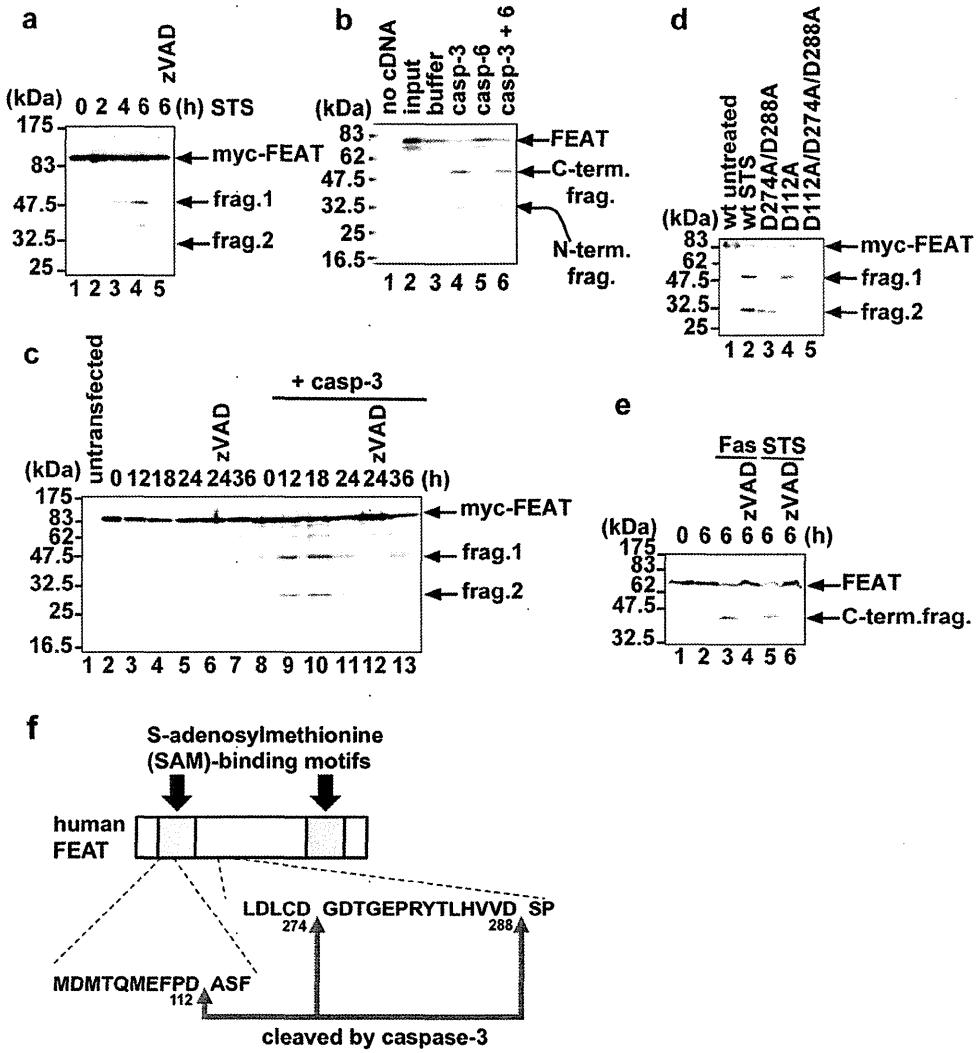

Figure 1 | FEAT is a substrate for caspase-3. (a) Cleavage of N-terminal Myc-tagged FEAT (myc-FEAT) in apoptotic cells. COS-7 cells expressing myc-FEAT were treated with 1 μM staurosporine (STS) for the indicated times. Lane 5: cells pretreated for 30 min with 100 μM zVAD-fmk, a broad spectrum caspase inhibitor. (b) *In vitro* transcribed/translated [^{35}S]-labelled FEAT was cleaved by purified caspase-3, but not by caspase-6. (c) Caspase-3 is mainly responsible for FEAT cleavages. MCF-7 cells expressing myc-FEAT alone or together with procaspase-3 (+ casp-3) were treated with 1 μM STS for the indicated times. (d) Mutating caspase-3 cleavage sites abrogates FEAT cleavages. COS-7 expressing wild-type (wt) or mutant myc-FEAT were treated for 6 h with 1 μM STS (lane 2 to 5). Immunoblots (a, c, d) were probed with an anti-Myc antibody. (e) Cleavage of endogenous FEAT in apoptotic cells. Jurkat T cells preincubated for 1 h without or with 100 μM zVAD-fmk were treated for 6 h with 100 ng/ml CH-11 agonistic anti-Fas antibody or 1 μM STS. The immunoblot was stained with the anti-FEATΔN antibody. (f) Schematic diagram of the human FEAT structure and caspase-3 cleavage sites.

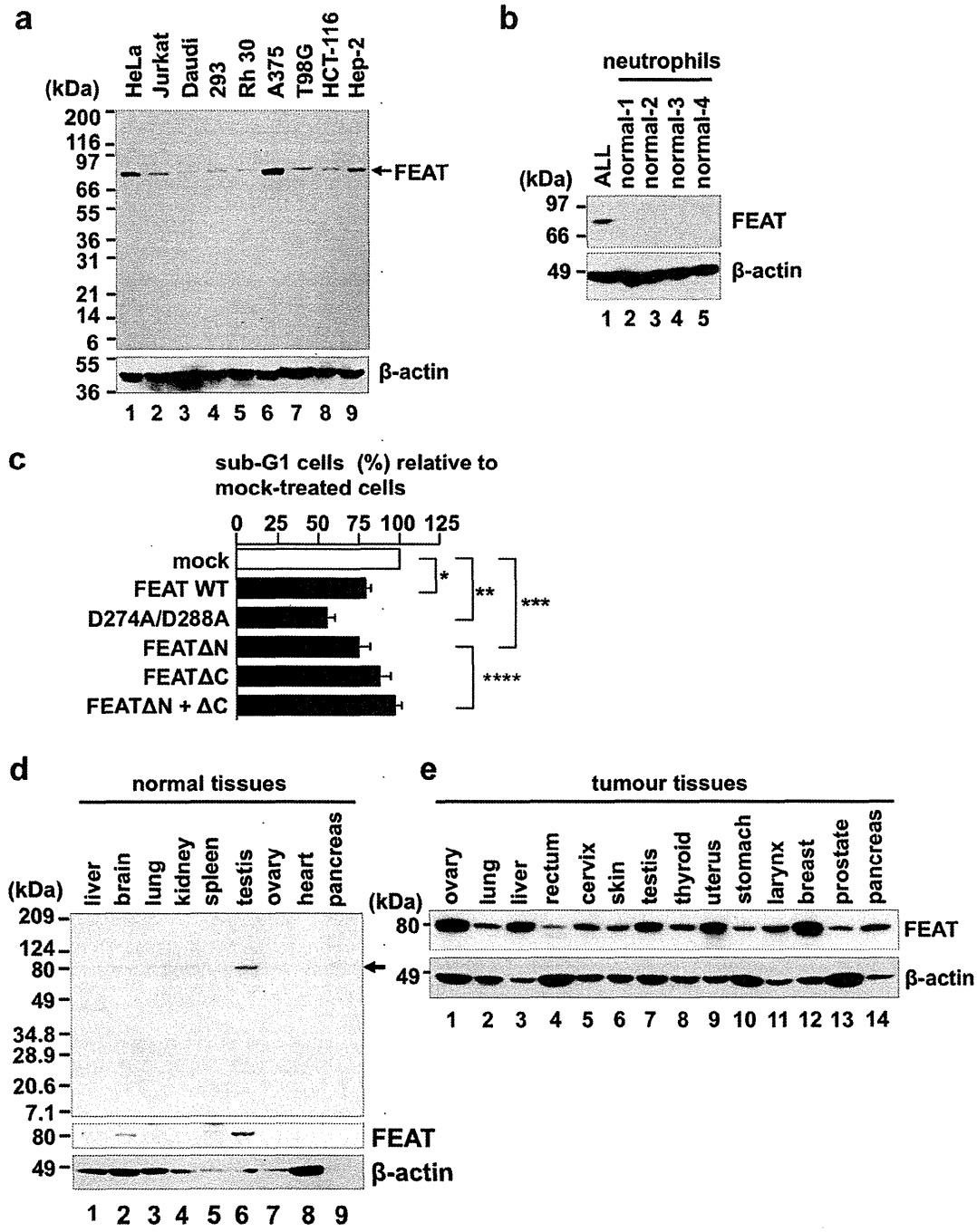

Figure 2 | FEAT is overexpressed in human cancers. (a) The immunoblot (IMB-105) contains lysates (10 μg protein/lane) from the following human cancer-derived cell lines: HeLa, uterine cervical carcinoma; Jurkat, T-cell leukaemia; Daudi, Burkitt lymphoma; 293, embryonal kidney transformed by adenovirus type 5; Rh 30, rhabdomyosarcoma; A375, malignant melanoma; T98G, glioblastoma; HCT-116, colon carcinoma; and Hep-2, larynx carcinoma. Immunofluorescence microscopy using the same antibody revealed that FEAT is diffusely localized in the cytoplasm and nucleus of HeLa cells (Supplementary Fig. 5; Supplementary Note). (b) Absence of FEAT expression in normal neutrophils. Peripheral blood mononuclear cells from a patient with acute lymphoblastic leukaemia (ALL) and neutrophils from four normal volunteers were analyzed by immunoblotting. (c) FEAT attenuates spontaneous neutrophil apoptosis. His-tagged wild-type (WT) or mutant FEAT proteins were introduced into neutrophils by protein transduction. Apoptotic neutrophils with a hypodiploid DNA content were analyzed by flow cytometry and normalized to that of cells incubated with irrelevant proteins (mock) (*, $P = 0.0012$, $n = 9$; **, $P = 0.0001$, $n = 9$; ***, $P = 0.0192$, $n = 4$; ****, $P = 0.0135$, $n = 4$; paired t-test). Error bars, s.e.m. (d) Multiple Tissue Blot (Human, WB46, 75 μg protein/lane) was probed with anti-FEATΔN (uppermost panel; FEAT is indicated by an arrow), anti-FEATΔC (middle panel), and anti-actin (lowermost panel) antibodies. (e) Human Tumor Tissue Blot (WB51). The proteins loaded (50 μg/lane) were derived from the following: ovary stromal sarcoma, lung adenocarcinoma, hepatocellular carcinoma, rectal adenocarcinoma, cervical squamous cell carcinoma, skin malignant melanoma, testis embryonal carcinoma, thyroid follicular carcinoma, uterine adenocarcinoma, stomach adenocarcinoma, laryngopharynx squamous cell carcinoma, breast ductal carcinoma, prostate hyperplasia, and pancreatic adenocarcinoma. (a, b, and e) Blots were probed with anti-FEATΔN (upper panels) and anti-actin (lower panels) antibodies.

studies are required to determine whether FEAT has enzymatic activities.

FEAT is cleaved by caspase-3. Exogenously-expressed FEAT was cleaved during staurosporine-induced (STS-induced) apoptosis of COS-7 cells (Fig. 1a). *In vitro* transcribed/translated FEAT was cleaved by caspase-3, but not by caspase-6 (Fig. 1b). Purified His-tagged FEAT was cleaved by purified caspase-3. FEAT was minimally cleaved in apoptotic MCF-7 cells, which are deficient in caspase-3 [26], and coexpression of procaspase-3 led to efficient cleavages of FEAT (Fig. 1c). Site-directed mutagenesis studies (Fig. 1d) revealed caspase-3 cleavage sites in human FEAT. Endogenous FEAT was cleaved in Jurkat T cells undergoing Fas- and STS-induced apoptosis (Fig. 1e). These results indicated that caspase-3 cleaves FEAT in apoptotic cells (Fig. 1f). D112 and D288 are well conserved across species (Supplementary Fig. 2; Supplementary Note), suggesting that caspase cleavages of FEAT play critical role(s) in organisms.

FEAT attenuates apoptotic cell death and the antiapoptotic activity is abrogated upon caspase-3-mediated cleavages. Cleavages of antiapoptotic kinases and phosphatases by caspases fine-tune apoptosis through terminating prosurvival signalling and generating proapoptotic peptide fragments [27]. We therefore assessed whether FEAT or its caspase-3-cleaved fragments affect apoptosis. *Ex vivo* experiments using plasmid transfection and RNA interference suggested that FEAT can impede apoptosis (Supplementary Fig. 4; Supplementary Note). We searched for cell types that do not express FEAT, found that almost all cancer-derived cell lines express FEAT (Fig. 2a), and decided to use neutrophils (Fig. 2b).

Protein transduction [28] of wild-type FEAT (FEAT WT) and FEATΔN (amino acid 289–699), a fragment generated by caspase-3 cleavage, significantly attenuated spontaneous apoptosis in neutrophils (Fig. 2c). The D274A/D288A mutant was more potent than FEAT WT or FEATΔN. In contrast, FEATΔC (amino acid 1–274), N-terminal fragment generated by the cleavage between the SAM-binding motifs, did not affect apoptosis, and the addition of FEATΔC interfered with the antiapoptotic function of FEATΔN (FEATΔN + ΔC). Taken together, the results are consistent with the notion that FEAT has the ability to attenuate apoptosis, which is abrogated by caspase-3 cleavages between the SAM-binding motifs.

FEAT is aberrantly overexpressed in human cancer tissues. We noticed that FEAT corresponds to the TGACCTCCAG tag that is used in the serial analysis of gene expression (SAGE) studies of human transcriptomes, which has been linked to a transcript that is uniformly elevated in human colon, brain, breast, and lung cancers and melanoma compared with the corresponding normal tissues [29]. Consistent with these classifications, immunoblotting analyses of normal human tissues showed weak FEAT expression only in the testis, brain, and liver (Fig. 2d), which correlated with mRNA expression [23]. In marked contrast, FEAT protein was moderately to highly expressed in a wide range of human cancer tissues (Fig. 2e), suggesting that FEAT is a ubiquitous protein involved in tumour biology.

FEAT upregulation is oncogenic *in vivo*. To assess whether FEAT upregulation in human cancers contributes to tumorigenesis, we generated transgenic mice that express human FEAT under a promoter that is active in a wide range of tissues (Supplementary Note). Immunoblotting showed expression of FEAT in the thymus, spleen, liver, and lung of transgenic mice (Fig. 3a). Thymocytes from transgenic mice showed significant decreases in Fas ligand- and glucocorticoid-induced cell death (Fig. 3b), indicating that transgenic expression of FEAT attenuates apoptosis.

After 12 month of age, the transgenic mice began developing hepatocellular carcinoma (HCC), as supported by immunohistochemical analyses of α-fetoprotein and albumin, and malignant lymphoma (Fig. 3c and Supplementary Fig. 6). HCC was also observed in a 9-month-old male transgenic mouse (Supplementary Fig. 6), suggesting that the hepatocarcinogenesis can be initiated earlier. In contrast, none of the nontransgenic littermates developed HCC, and lymphoma was observed in nontransgenic littermates with a lower incidence (18%, 3/17). Consequently, the transgenic mice developed tumours or died earlier than the nontransgenic littermates (Fig. 4a). HCC and lymphoma were observed in the offspring of four distinct founders (Fig. 3c), arguing against the possibility that the tumorigenesis resulted from integration of the transgene in endogenous cancer genes in the mouse genome. The murine HCC recapitulated the strong male predilection (Fig. 3c) that is observed in human patients [30].

Murine HCCs displayed various histological subtypes similar to human HCCs (Fig. 4b). Lung metastases were detected in two mice with HCC (Fig. 4c). Most lymphomas belonged to diffuse large or Burkitt-like B-cell lymphoma (Fig. 5a), both of which expressed the B-cell marker CD45R (B220) (100%, 15/15) (inset) and had undergone clonal rearrangement of the immunoglobulin genes (83%, 5/6). These are the types of lymphoma that are most common in human patients. None of the examined lymphomas were positive for the T-cell marker CD3 (0%, 0/7). CD45R- and CD3-negative polymorphic variants with giant cells were also observed (Fig. 5b). The lymphomas were highly invasive and often infiltrated the pancreas (Fig. 5c).

One transgenic mouse developed both HCC and lymphoma (Fig. 5d), and another transgenic mouse harboured three tumours, i.e., lymphoma, HCC, and lung adenocarcinoma (Fig. 5e), as confirmed by the expression prosurfactant protein C (insets). In addition, one mouse had lymphoma and rhabdomyosarcoma (Supplementary Fig. 6). Immunohistochemistry showed that FEAT expression is higher in HCCs than adjacent liver tissues. Sequencing analyses showed that there were no mutations in the FEAT transgene in HCCs (0%, 0/5), suggesting that structural changes in FEAT are not required for tumorigenesis. Unlike the CF-1 and C3H inbred strains, the occurrence of HCC is unusual in C57BL/6 mice [31]. Thus, FEAT is a unique oncoprotein that potently induces both HCC and malignant lymphoma on the C57BL/6 inbred strain background.

FEAT transgenic mice as a relevant model for human HCCs. Mouse models of cancers with extensive physiological and molecular similarities to human patients can be exploited to determine the causes of human cancers, to devise the strategy for cancer prevention, and to develop and test new treatments [32]. Inflammation plays critical roles in the initiation and promotion of human and murine HCCs [33]. To evaluate the possibility that FEAT promotes hepatocarcinogenesis by inducing prolonged inflammatory responses such as autoimmune hepatitis, we examined whether FEAT transgenic mice with HCC have background inflammatory lesions in the liver. Only sparse low-grade perivasculitis with minimal tissue destruction was observed in 50% (7/14) of the liver adjacent to HCC in FEAT transgenic mice, while a similar degree of perivasculitis was detected in 35% (6/17) of the liver from nontransgenic littermates (Supplementary Fig. 7). The observations did not support the idea that FEAT causes HCC through inflammatory mechanisms.

We next assessed whether the HCCs in FEAT transgenic mice closely model genetic events in human HCCs. The loss of p53 tumour suppressor function is a key event in certain subsets of human HCCs [34]. In particular, HCCs caused by aflatoxin characteristically have the S376A mutation in p53. Mutations in the open reading frame (ORF) of the p53 mRNA were not detected in mouse HCCs (0%, 0/7). MDM2 amplification, which is observed in some human HCCs [35], was unlikely

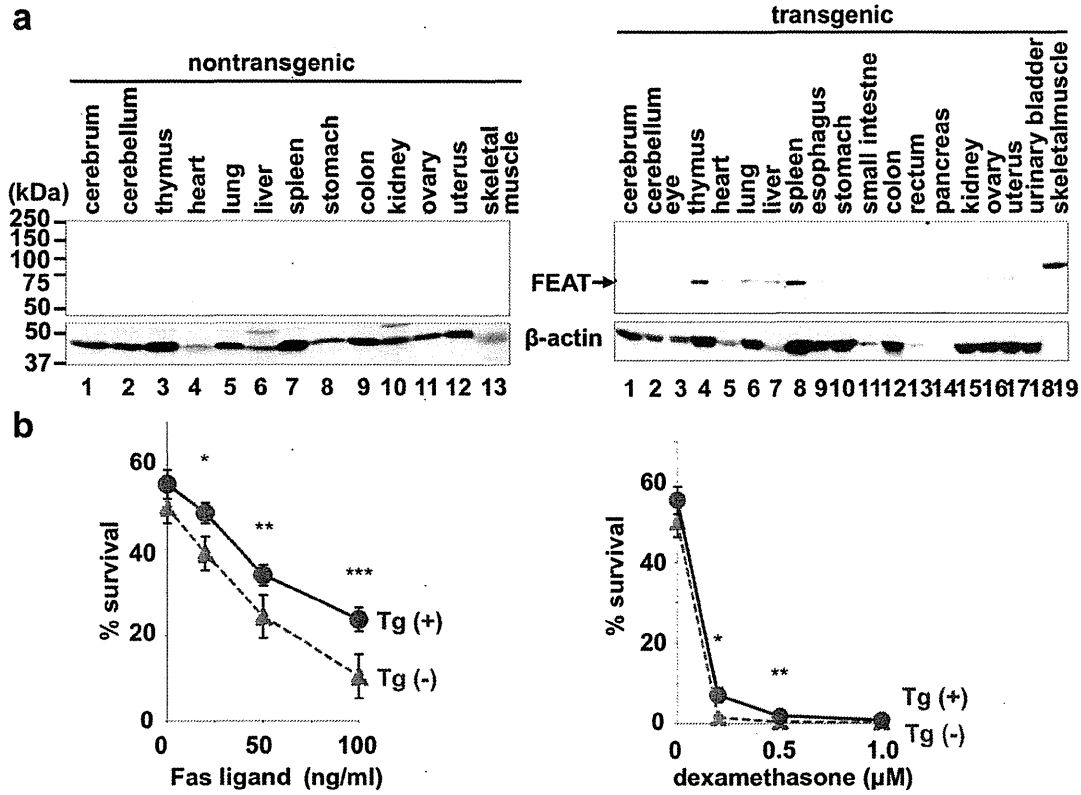

c

mouse lines	1 (n = 7)	10 (n = 1)	14 (n = 1)	16 (n = 12)	18 (n = 12)	23 (n = 7)
age at analyses (months)	9-28	27	28	18-27	12-23	18-30
HCC	3	0	0	4	6	1
lymphoma	1	1	1	5	6	6
other tumour	0	0	0	2	0	1
non-tumour death	3	0	0	2	1	1

	male (n = 26)	female (n = 14)
age at analysis (months)	9-30	17-28
HCC	13 (50%)	1 (7.1%)
lymphoma	10 (38%)	10 (71%)
other tumours	1 (3.8%)	2 (14%)
non-tumour death	5 (19%)	2 (14%)

Figure 3 | Analyses of FEAT transgenic mice. (a) FEAT protein expression in nontransgenic (left panel) or transgenic (right panel) mouse organs. Similar results were obtained with first generation offspring of three distinct founders. The blot (30 μg protein/lane) was probed with anti-FEATΔN (upper panels) and anti-actin (lower panels) antibodies. (b) Cell death of thymocytes is attenuated in FEAT transgenic mice. Survival of thymocytes isolated from transgenic mice (Tg (+)) (red, solid lines) or nontransgenic littermates (Tg (-)) (blue, dashed lines) were analyzed by flow cytometry (means ± s.e.m.) after treatment for 24 h with Fas ligand (left panel) (*, $P = 0.02492$; **, $P = 0.0497$; ***, $P = 0.0226$, $n = 5$; paired t-test) or dexamethasone (right panel) (*, $P = 0.0331$; **, $P = 0.0411$, $n = 6$; paired t-test). (c) Tumours in founder, first and second generation FEAT transgenic mice. HCC, hepatocellular carcinoma.

because immunohistochemistry did not reveal increased MDM2 in the mouse HCCs compared with adjacent normal liver tissues (0%, 0/5). Activation of Wnt signalling pathway through mutations in ß-catenin or Axin that is found in a small population of human HCCs [36] was unlikely because of the absence of the nuclear localization of ß-catenin (0%, 0/6) and of any mutations in the hotspots in the ß -catenin gene (0%, 0/9). Overall, HCCs in the transgenic mice do not correspond to certain minor subsets of human HCCs [36].

To evaluate whether the mouse HCCs harbour chromosomal changes similar to human patients, the amplification (gain) or deletion (loss) of genomic regions (copy number alterations, CNAs) were analyzed by microarray-based comparative genomic hybridization (array-CGH). A genome-wide view of large-scale CNAs showed that the murine HCCs had marked genomic instability, with more gains than losses (Supplementary Fig. 8) as observed in human HCC [37], while the liver from a transgenic mouse without HCC had minimal

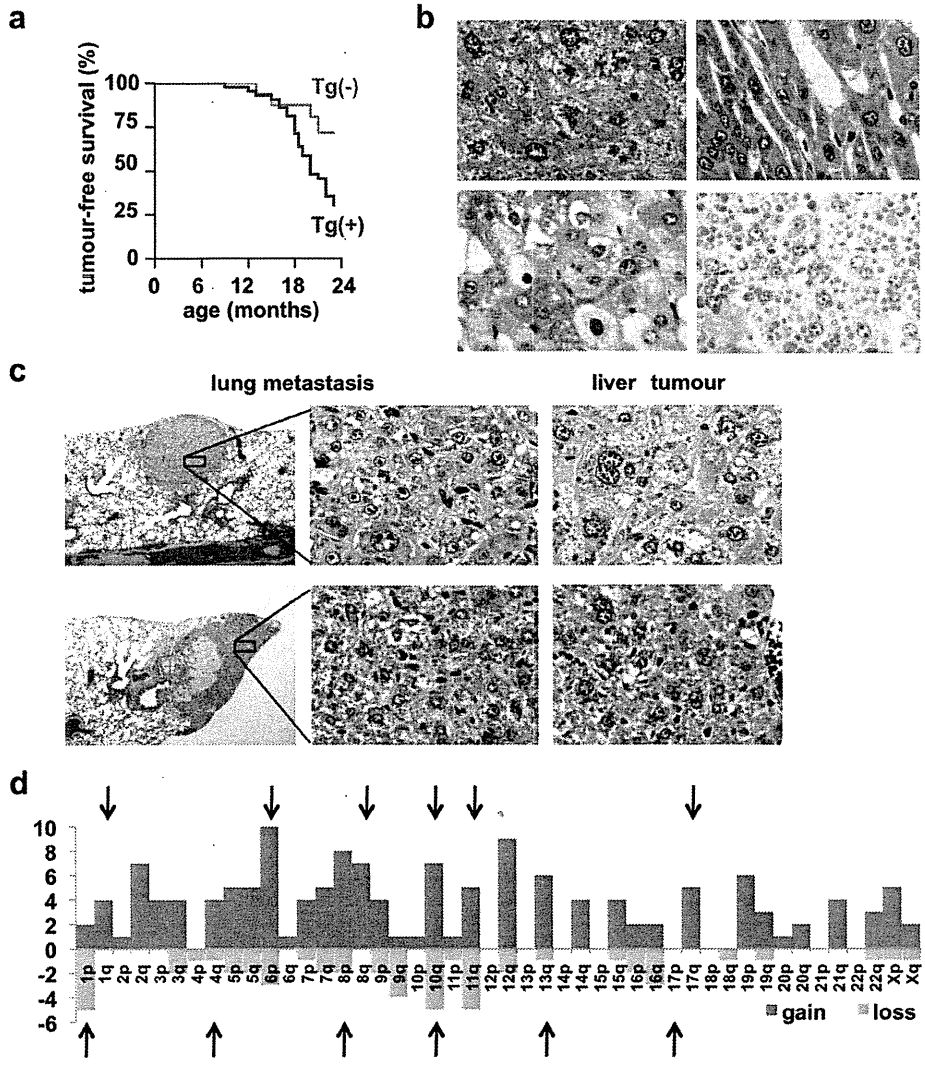

Figure 4 | Hepatocellular carcinoma (HCC) in FEAT transgenic mice. (a) Kaplan-Meier curve for tumour-free survival of FEAT transgenic mice (Tg (+)) (red) ($n = 40$) and nontransgenic littermates (Tg (-)) (blue) ($n = 17$) ($P = 0.038$, log-rank test). (b) Various histological subtypes of HCC. Well-differentiated tumours composed of dysplastic hepatocytes with atypical large polyploid nuclei and anisokaryosis with compact (upper left panel) and trabecular (upper right panel) growth patterns, and variants such as a clear-cell type (left lower panel) and HCCs with cytoplasmic inclusion bodies (right lower panel). (c) Morphology of neoplastic cells in lung metastases, which were similar to primary liver tumours. (b and c) hematoxylin and eosin (H&E) staining. Original magnifications are: ×115 (c, left panels) and ×600 (b; c, middle and right panels). (d) Syntenic human chromosomal regions corresponding to CNAs detected by array comparative genomic hybridization (array-CGH). Each column shows the number of genes present in each human chromosomal arm that was commonly gained (red) or lost (green) in HCCs of FEAT transgenic mice ($n = 6$). The arrows indicate the chromosomal arms that are gained or lost in human HCCs [41].

CNAs. This suggested that genomic fragility developed during the process of hepatocarcinogenesis rather than because of direct effects of the FEAT transgene.

Tandem duplications that range in size from 3 kb to greater than 1 Mb is the most commonly observed architectures of rearrangement in a recent study of human breast cancer genomes [12]. High-resolution array-CGH revealed gain or loss of such small chromosomal segments in the murine HCCs. The small-scale CNAs involved 18 known cancer genes (http://www.sanger.ac.uk/genetics/CGP/Census/) (*MDS1, PDGFRA, PIK3R1, JAZF1, WHSC1L1, HOOK3, PCM1, MLLT3, PTEN, CBL, ERCC5, ERCC4, CYLD, CBFB, BRIP1, MLLT1, TMPRSS2, NF2*) (Supplementary Table 1). *TTN* [4], *SKP2* [38], *EED1* [39], and *PVT1* [40] have also been implicated in oncogenesis. To directly compare the small-scale CNAs in mouse and human HCCs, we listed focal CNAs that were shared among the murine HCCs and identified human chromosomal loci syntenic to the CNAs (Supplementary Table 1). The syntenic regions covered most of the chromosomal changes that were previously implicated in human HCCs [41] (Fig. 4d) and exhibited marked similarities with array-CGH data of human HCCs [37]. This cross-species synteny implies that the carcinogenesis in these mice closely mimics that in human patients and indicates that the FEAT transgenic mouse may be a highly relevant model of human HCCs [42].

Molecular bases for oncogenic functions of FEAT. The oncogenic potential of FEAT in transgenic mice seemed to be disproportionate to the moderate ability to attenuate apoptosis (Fig. 2c, Fig. 3b, and Supplementary Fig. 4). NIH3T3 cells that overexpressed FEAT, FEATΔN, or FEATΔC did not consistently form colonies in soft agar, suggesting that the assay for anchorage-independent growth can fail to detect potently tumorigenic genes. This supported the limitation of *ex vivo* screening for cancer genes and the much

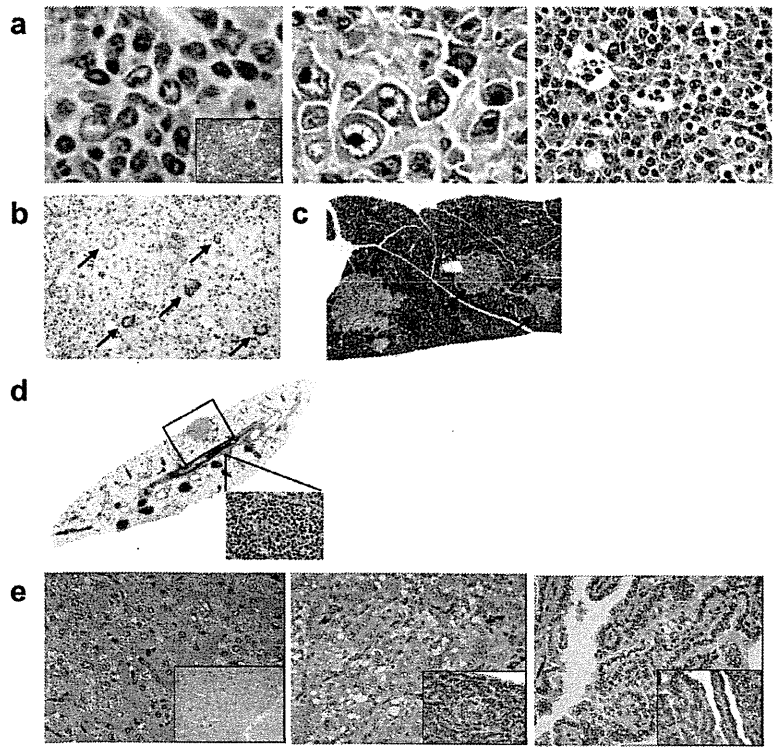

Figure 5 | Lymphoma and co-occurrence of other tumours in FEAT transgenic mice. (a) Microscopic appearance of B-cell lymphomas from FEAT transgenic mice. Centroblastic (left panel) or immunoblastic (middle panel) variants of diffuse large B-cell lymphoma and Burkitt-like B-cell lymphoma with a starry sky appearance (right panel). (b) Giant cells (arrows) in polymorphic lymphoma. (c) Infiltration of lymphoma in the pancreas (arrows). (d) A section of the lung with metastases of hepatocellular carcinoma (HCC) (rectangle, corresponding to left upper panel in Fig. 4c) and lymphoma (inset). (e) HCC (left panel), and a lung adenocarcinoma (middle and right panels) that developed in a transgenic mouse, which also harboured lymphoma. (a–e) H&E staining. Original magnifications are: ×600 (a), ×115 (b), ×60 (c), ×15 (d), and ×400 (e). The insets show immunohistochemical staining for a B-cell marker CD45R (B220) (a), and prosurfactant protein C, a marker of type II pneumocytes, which was absent in the HCC and present in the lung adenocarcinoma (e).

broader relevance of genetic engineering and *in vivo* analyses of mice [19].

To evaluate whether FEAT has cellular functions relevant in oncogenesis, FEAT was overexpressed in NIH3T3 cells, which only weakly express FEAT protein (Fig. 6a), and the alterations in genome-wide transcriptional profiles were analyzed by microarrays. Gene set enrichment analysis (GSEA) [43] revealed that FEAT overexpression increases the signatures of receptor tyrosine kinase (RTK) and hedgehog signalling pathways (Fig. 6b and Supplementary Table 2), which are known to play major roles in the development and maintenance of cancers [44–46]. The results suggested that the ability to drive multiple oncogenic pathways underlies the robust tumorigenic potential of FEAT *in vivo*.

FEAT is upregulated in most human cancer cells. Previous studies using expression microarrays reported that FEAT (KIAA0859, CGI-01) mRNA is upregulated in uterine and ovarian cancers (http://www.freepatentsonline.com/20050244843.html), superficial bladder cancer (https://www.oncomine.org), adenocarcinomas of the stomach [47], and retinoblastoma [48]. To further assess the range of human cancers in which FEAT may be involved in oncogenesis, we examined FEAT levels in various human cancers and their subtypes using Tissue Arrays. Immunohistochemistry detected significant upregulation of FEAT in colon (46%, 17/37), pancreatic (61%, 11/18), prostate (39%, 7/18), breast (51%, 18/35), ovary (24%, 6/25), thyroid (47%, 9/19), and non-small-cell lung cancers (64%, 14/22) (Fig. 7 and Supplementary Fig. 9; Supplementary Table 3). FEAT was upregulated in cancer cells but not nonneoplastic stromal cells or normal cells adjacent to cancer tissues. Thus, FEAT upregulation is common and widespread in human cancers, suggesting that this phenomenon is a fundamental process in the development of most cancers.

Notably, FEAT overexpression can also precede neoplastic transformation in human HCCs; hepatocytes that were adjacent to HCC in liver cirrhosis expressed high levels of FEAT (Fig. 8), most likely reflecting ongoing carcinogenesis in these cirrhotic livers. FEAT overexpression was also observed in intraductal carcinoma *in situ* of breast (Supplementary Fig. 9) [49], an early phase preceding invasion. These observations suggest that FEAT functions from preneoplastic or early neoplastic processes of diverse human cancers.

Discussion

One of the most feasible and promising approaches for cancer prevention and screening is to target a common event that occurs in most tumours. Despite these potential therapeutic advantages, it is still poorly understood whether a crucial molecular event commonly occurs in the early oncogenesis of most cancers. The present study demonstrates that an unrecognized protein, FEAT, is highly oncogenic *in vivo*. Remarkably, this prominent promoter of tumorigenesis is aberrantly overexpressed in most human cancers starting in the early phases of tumorigenesis. Chromatin immunoprecipitation studies with mouse embryonic stem cells (ESCs) indicate that oncogene products such as c-Myc [50–52], N-Myc [51], and E2F1 [51] are bound to the promoter of the mouse *Mettl13* gene (also known as *5630401D24Rik*). Amplicons in various cancers including HCC [37], malignant lymphoma, and high-risk multiple myeloma (http://www.freepatentsonline.com/y2008/0274911.html) involve the

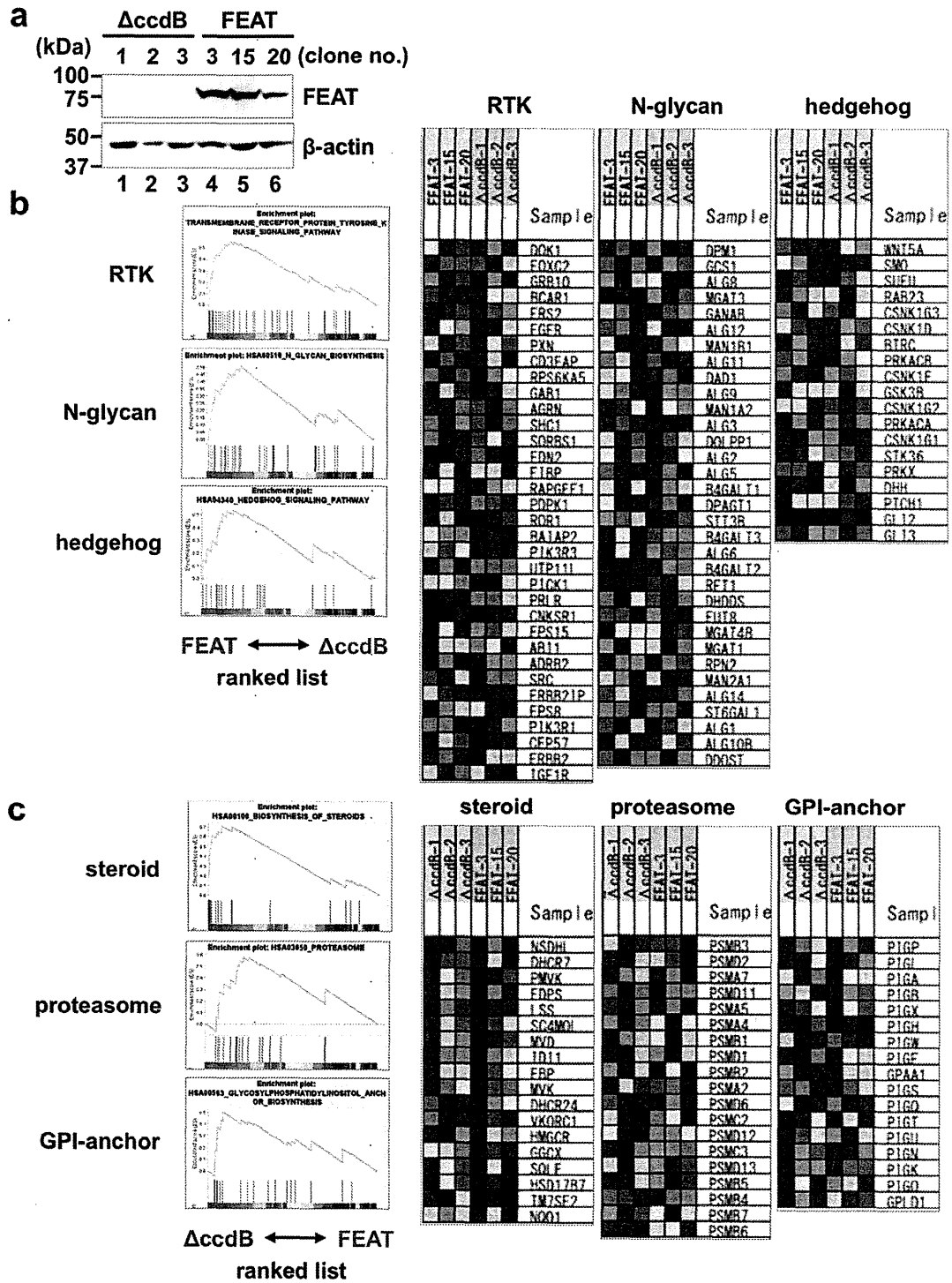

Figure 6 | Genome-wide expression profiling of NIH3T3 cells overexpressing human FEAT. (a) Immunoblot analyses of NIH3T3 cell clones stably transfected with a control plasmid (ΔccdB-1, ΔccdB-2, and ΔccdB-3) and human FEAT cDNA (FEAT-3, FEAT-15, and FEAT-20). The blot was probed with anti-FEATΔN (upper panel) and anti-actin (lower panel) antibodies. Signatures enriched in FEAT-overexpressing (FEAT-3, -15, and -20) (b) or control (ΔccdB-1, -2, and -3) (c) NIH3T3 cells as assessed by gene set enrichment analysis. Enrichment plots (left panels) and heat maps (right panels) display gene sets with enrichment score (ES) > 0.5 and false discovery rate (FDR) q-value < 0.25. RTK, receptor tyrosine kinase. GPI, glycosylphosphatidylinositol.

human *METTL13* gene at 1q24.3. These observations might explain how FEAT protein is upregulated in tumours. Further studies are needed to fully elucidate the regulation of FEAT expression in normal and neoplastic tissues.

FEAT was originally purified from rat livers as a protein that inhibits nuclear apoptosis *in vitro*. Interestingly, FEAT homologues were not detectable in unicellular eukaryotes such as yeasts and green algae (*Chlamydomonas reinhardtii*), suggesting that the functions of

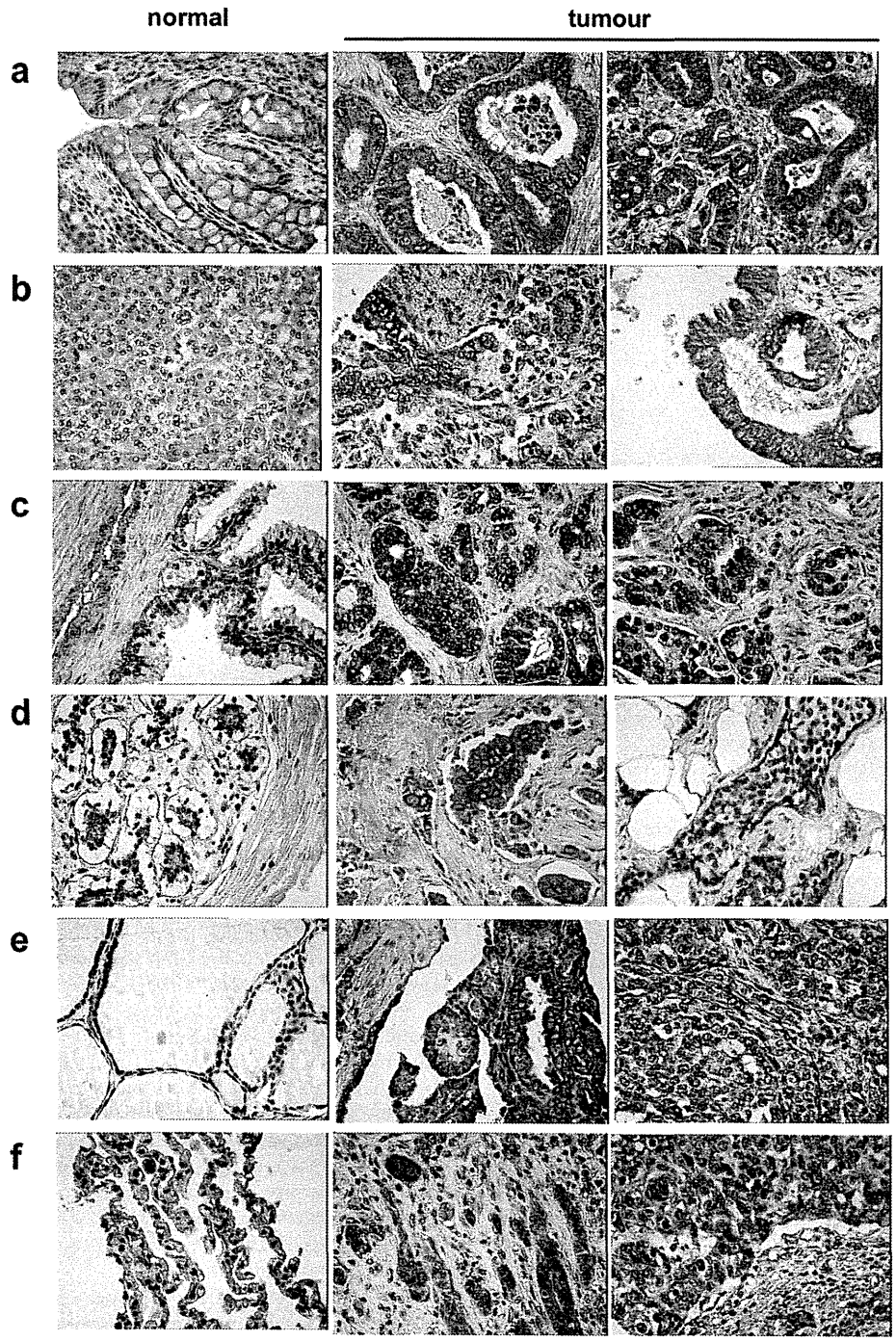

Figure 7 | Overexpression of FEAT in diverse human cancer cells. Immunohistochemical staining of Tissue Arrays using anti-FEAT ΔN antibody. (a) Normal colon tissue, grade I and III adenocarcinoma of the colon. (b) Normal pancreas tissue, grade I and II adenocarcinoma of the pancreas. (c) Normal prostate tissue, Gleason score 1 and 3 adenocarcinoma of the prostate. (d) Normal breast tissue, infiltrating ductal and lobular carcinomas of the breast. (e) Normal thyroid tissue, grade I papillary and grade III follicular carcinomas of the thyroid. (f) Normal lung tissue, grade III adenocarcinoma and grade III squamous cell carcinoma of the lung. Original magnification: × 400. The following Tissue Arrays were used: High density multiple organ cancer and normal tissue microarray, MC5001; Breast cancer tissue microarray with self-matching adjacent normal tissue and normal tissue controls, BR721; Colon adenocarcinoma (combination of marginal and normal), BC05021; and Liver carcinoma (combination of cancer, cancer adjacent and normal tissue), LV803.

FEAT are unique to multicellular organisms. Interestingly, mouse FEAT belongs to the Myc module in mouse ESCs that is responsible for the similarity between ESCs and cancer cells [53], implicating FEAT as a link between cancer and stem cell biology. *Ex vivo* experiments confirmed that FEAT attenuates apoptotic cell death. However, gene expression profiling revealed that FEAT also affects various cell signalling and metabolic pathways (Fig. 6b and 6c; Supplementary Table 2). Furthermore, in a recent genome-wide linkage analysis, genetic variations in the human *METTL13* gene have been associated with increased susceptibility to postpartum mood syndrome [54]. CpG-island microarray analyses of frontal cortex tissues have revealed higher DNA methylation close to the *METTL13* gene among bipolar

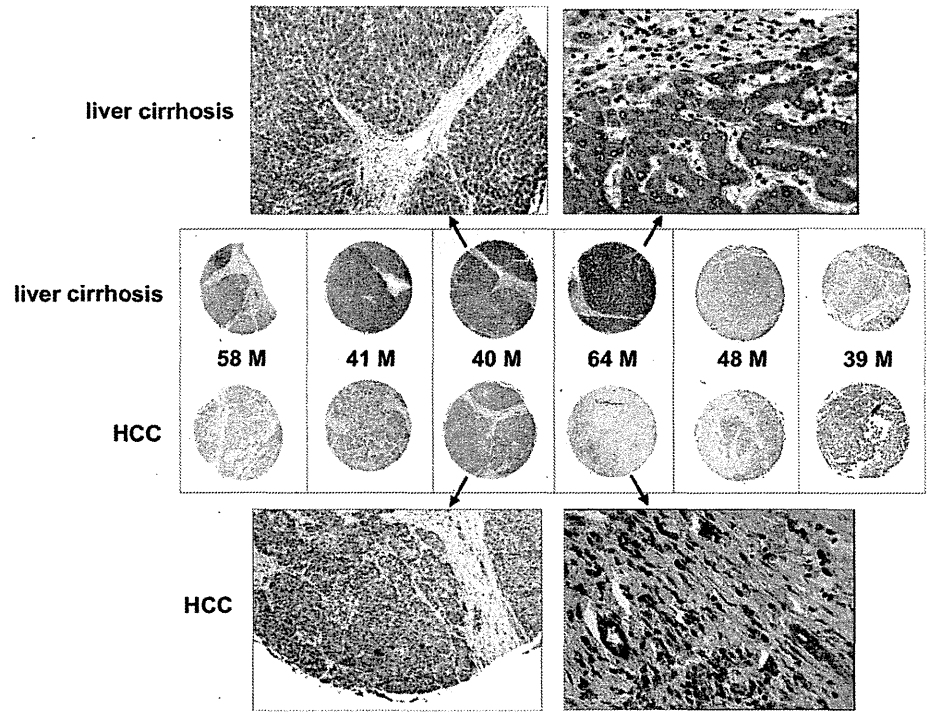

Figure 8 | FEAT is overexpressed in liver cirrhosis adjacent to human hepatocellular carcinoma (HCC). FEAT expression in HCC and the adjacent cirrhotic liver was compared for several patients using a Tissue Array (LV803). The age and gender (M, male) of the patients are indicated. Original magnifications are: ×115 (left uppermost panel, left lowermost panel), ×400 (right uppermost panel, right lowermost panel), and ×40 (middle panels).

disorder females and psychosis females [55]. Therefore, it will be important to perform integrated studies to fully elucidate how the multifunctional properties of FEAT contribute to tumorigenesis.

A potential problem with transgenic mouse models of cancer is that the transgene is expressed throughout the entire organ, while human cancers are thought to develop from a single mutated cell in the context of a relatively normal organ [32]. FEAT transgenic mice did not have the premalignant lesions (ex. steatohepatitis, cholestatic hepatitis, and liver fibrosis) that typically precede HCCs in other mouse models and human patients with underlying hepatitis B or C virus infections, alcoholic liver injury, or nonalcoholic steatohepatitis [41]. Thus, a possible limitation of the FEAT transgenic mouse model is that it cannot recapitulate the inflammatory mechanisms that underlie most human HCCs. Inflammatory responses leading to STAT3 signalling downstream of interleukin-6 have been implicated in the development of murine and human HCCs [33]. Whereas FEAT induces malignant HCCs in mice that can metastasize to the lung, constitutive interleukin-6-STAT3 signalling can only induce benign hepatic adenomas [56], suggesting that the inflammatory mechanisms play central roles mainly at earlier phases in the evolution of HCCs. Immunohistochemical analyses of Tissue Arrays from human patients revealed that FEAT is diffusely overexpressed in hepatocytes in liver cirrhosis adjacent to HCC. FEAT upregulation in transgenic mice may bypass the preneoplastic processes that precede advanced liver cirrhosis. In compensation for the inability to recapitulate the earlier inflammatory phases of hepatocarcinogenesis, FEAT transgenic mice may help us investigate a 'pure' later phase of carcinogenic processes that are not complicated by genetic alterations that are secondary to the preceding processes [57].

The relatively delayed development of HCC and lymphoma in transgenic mice (Supplementary Fig. 6) implies that FEAT is involved in promoting, rather than initiating oncogenesis. The genomic instability that was indicated by the array-CGH also suggests that multiple additional genetic alterations are required for tumorigenesis. The incidence of tumours in transgenic mouse lines was not correlated with differences in FEAT transgene expression among these lines ($1 > 16 > 23 \gg 18$), suggesting that the level of FEAT protein is not a rate-limiting factor in tumorigenesis. In addition, Tissue Arrays showed no correlation between FEAT levels and tumour grades. Downregulation of FEAT in human HCC compared to the adjacent cirrhotic liver and the moderate ability of FEAT to attenuate apoptotic cell death in HeLa cells suggested that FEAT is not necessary to maintain cancers. Taken together, these results indicate that FEAT upregulation potently promotes the development of multiple tumours *in vivo*, mainly at the prodromal and early phases of carcinogenesis, and sets the stage for additional oncogenic processes. Spontaneous lymphoma, HCC, lung cancer, and rhabdomyosarcoma can occur in C57BL/6 mice, albeit at low rates. The occurrence of these specific types of tumours suggests that the FEAT transgene promoted the intrinsic tendency of C57BL/6 mice to develop tumours such as lymphoma. Therefore, it is likely that FEAT accelerates and enhances the intrinsic predispositions of certain humans to develop cancers.

Biochemical events that are common among cancers have been used to screen or monitor tumour development, spread, and viability, as exemplified by positron emission tomography (PET) for glucose uptake. Compared to alterations in other oncogenes and tumour suppressor genes [15], FEAT is upregulated in an unusually wide range of tumours. Moreover, Tissue Array analyses demonstrate that FEAT upregulation can be easily examined using formalin-fixed paraffin-embedded sections that are available in most community hospitals. MUC1 [58] and survivin [59], which are overexpressed in diverse cancers, are currently being examined as targets for immunotherapy in clinical trials. Immunization with FEAT may trigger immune responses that eradicate precancerous lesions and early-stage tumours, preventing further development of invasive and metastatic cancers. Thus, FEAT might become the prototype of a subfamily of cancer genes that could lead to new methods for cost-effective cancer screening and prevention. The results of our study suggest that we should further explore FEAT-like ubiquitous

oncoproteins and exploit the molecular features of these proteins in various clinical applications.

Methods

Reagents. Benzyloxycarbonyl-Val-Ala-Asp(OMe)-fluoromethylketone (zVAD-fmk) was obtained from Enzyme Systems. The pcDL-SRα-procaspase-3 plasmid was kindly provided by Dr. Fumiko Toyoshima-Morimoto (Institute for Virus Research, Kyoto University, Kyoto, Japan). The agonistic anti-Fas IgM monoclonal antibody (CH-11) was purchased from MBL. The INSTA-Blot membrane (IMB-105) was obtained from IMGENEX. Multiple Tissue Blot (Human) (WB46) and Human Tumor Tissue Blot (WB51) were obtained from Calbiochem (Merck). Tissue Arrays that were spotted with an array of formalin-fixed and paraffin-embedded specimens derived from various normal and tumour tissues were purchased from US Biomax.

Antibodies. The following primary antibodies were used: rabbit polyclonal antibodies against actin (A5060; Sigma), human c-Myc (Anti-Myc Tag, 06-549; Upstate, Millipore), albumin (A0001; DakoCytomation Denmark A/S), and prosurfactant protein C (AB3786; Chemicon International, Millipore); mouse monoclonal antibodies against human c-Myc (9E10; sc-40), HA (Y-11; sc-805), MDM2 (sc-965) (Santa Cruz Biotechnology), α-fetoprotein (AB3786; Vector Laboratories), and ß-catenin (610153; BD Transduction Laboratories, BD Biosciences).

Rabbit polyclonal antibodies against human FEATΔN and human FEATΔC were produced and affinity-purified by Operon Biotechnologies (Tokyo, Japan). Detailed characterization of the antibodies is described in Supplementary Methods.

Determination of caspase cleavage sites. The candidate aspartic acid residues encoded by FEAT cDNA in the pBluescript SK(-) plasmid (Stratagene) were mutated to alanine using the GeneEditor *in vitro* Site-Directed Mutagenesis System (Promega). *In vitro* transcription/translation of the cDNAs was performed using the TNT T7/T3 Coupled Reticulocyte Lysate System (Promega) and Tran^{35}S-label (MP Biomedicals). The [^{35}S]-labelled recombinant wild-type or mutant FEAT proteins were incubated with purified recombinant caspase-3 for 2 h at 37°C, resolved by sodium dodecyl sulphate polyacrylamide gel electrophoresis (SDS-PAGE), and visualized by autoradiography.

Isolation of neutrophils, protein transduction, and analysis of spontaneous apoptosis. The PTD-4 sequence (YARAAARQARA) optimized for protein transduction [60] was introduced between the His-tag and N-terminus of the wild-type or mutant FEAT proteins. The proteins encoded by the pET-16b plasmids (Novagen, Merck) were expressed in BL21(DE3)pLys *Escherichia coli* (Novagen, Merck) and purified with Ni^{2+}-NTA agarose (Qiagen) under denaturing conditions.

Neutrophils were isolated from the peripheral blood of healthy adult volunteers using two-step Percoll (GE Healthcare Bio-Sciences) gradients. Neutrophils were resuspended in RPMI-1640 medium (Sigma) supplemented with 10% FBS (GIBCO, Invitrogen, Life Technologies), 50 U/ml penicillin, and 50 μg/ml streptomycin (GIBCO, Invitrogen, Life Technologies) (FBS-RPMI) and then treated with 1 μM of the purified proteins for 15 min at 37°C. After the treatment, the cells were diluted with FBS-RPMI and then incubated for 24 h at 37°C. Neutrophil apoptosis was assessed by ethanol fixation, propidium iodide staining, and analyses of the cells with hypodiploid DNA content using the FACScan flow cytometer and CellQuest software (BD Biosciences). Cell death was also confirmed by flow cytometric analyses of cells stained with fluorescein isothiocyanate-conjugated (FITC-conjugated) annexin V and propidium iodide using the ApoAlert annexin V Apoptosis Detection kit (Clontech Laboratories, Takara Bio).

Generation and breeding of FEAT transgenic mice. All animal experiments were approved by the Animal Experiment Committee at the Chiba Cancer Center. Injection of the DNA fragment containing the H-2K^d (MHC Class I) promoter, FEAT cDNA, β-globin intron, and SV40 poly (A) signal into fertilized eggs collected from superovulated C57BL/6CrSlc females, implantation into pseudo-pregnant mice, breeding, and weaning were performed by Japan SLC (Shizuoka, Japan).

The founder mice were screened for integration of human FEAT cDNA by Southern blotting using genomic DNA purified from tails. Briefly, 0.5 cm of mouse tails were incubated overnight at 55°C in 0.5 ml lysis buffer (10 mM TrisHCl, pH 7.5, 50 mM ethylenediamine tetraacetic acid (EDTA), 0.5% SDS, 100 mM NaCl, and 100 μg/ml proteinase K). After adding 0.5 ml UltraPure phenol:chloroform:isoamyl alcohol (Invitrogen, Life Technologies), the samples were rotated for 30 min at room temperature, and then centrifuged for 2 min at 7,000 rpm. The aqueous phase was recovered and treated similarly with 0.5 ml chloroform. The genomic DNA was precipitated by adding 0.4 ml isopropanol, and then washed with 70% ethanol and dissolved in 0.2 ml TE buffer (10 mM TrisHCl, pH 8.0, and 1 mM EDTA). After digesting with *Bam*HI and capillary transfer to Nytran SuPerCharge nylon membranes using the TurboBlotter Rapid Downward Transfer Systems (Schleicher & Schuell Bioscience, Whatman, GE Healthcare Bio-Sciences), the integrated cDNA was detected using the AlkPhos Direct Labeling and Detection System (GE Healthcare Bio-Sciences).

Thereafter, expression of the transgene in each mouse was determined by polymerase chain reaction (PCR) analysis using DNA isolated from the tail by a simplified protocol. Briefly, 0.5 cm of tail was incubated overnight at 55°C in 100 μl lysis buffer (20 mM TrisHCl, pH 7.5, 100 mM EDTA, 0.5% Tween-20 (Bio-Rad), and 100 μg/ml proteinase K), followed by the addition of 900 μl distilled water. For a 20 μl PCR reaction using KOD Dash DNA polymerase (TOYOBO), 0.5 μl of the lysate was used as a template with the following primers: 5′-TGGCTCTTTGGCATGGATGA-3′ (forward) and 5′-TATGACATCGTAGCAAGGCC-3′ (reverse). Sperm were obtained from the epididymides of transgenic mice and cryopreserved by Kyudo Co., Ltd. (Tosu, Japan).

Transgenic mice and their nontransgenic littermates were bred and maintained in a specific pathogen-free (SPF) animal facility at the Chiba Cancer Center Research Institute. Transgenic lines were maintained by crossing male transgenic mice to normal female C57BL/6 mice (Charles River Laboratories). Mice that had tumours or were in a moribund state were euthanized and necropsied.

Apoptotic cell death of mouse thymocytes. Thymocytes were isolated by grinding the dissected thymus with the plunger of a 1-ml sterile syringe in FBS-RPMI at room temperature. The cells were left untreated or treated with Fas ligand (rhs*Super*FasLigand) (Alexis) or dexamethasone (Nacalai Tesque) for 24 h at 37°C in a humidified atmosphere containing 5% CO_2. Cell death was quantified by staining the cells with annexin V-CFS (R&D Systems) and propidium iodide (Calbiochem, Merck), and then analyzing the cells by flow cytometry.

Microscopic analyses of mouse tissues. After dissection, the mouse organs were fixed with 3.7% formaldehyde in phosphate-buffered saline, sliced into 2-mm thick sections, placed into tissue cassettes (Tissue-Tek Uni-Cassette; Sakura Finetek Japan), and immersed in fresh fixative. Further processing and interpretation of the microscopic pathology were performed by Narabyouri Research Co., Ltd. (Nara, Japan). Briefly, fixed tissues were dehydrated through a series of ethanol (20% to 100%) and xylene solutions and embedded in paraffin using an automatic tissue processor, sectioned with a microtome, deparaffinized, rehydrated, and stained with hematoxylin and eosin (H&E). Immunohistochemical staining for CD45R (B220) and CD3 was performed with an Autostainer (DAKO).

Array-CGH. The quality of genomic DNA was assessed by electrophoresis of 200 ng DNA on a 0.8% agarose gel containing 0.5 μg/ml ethidium bromide. Only DNA preparations without smearing were used for subsequent steps. DNA labelling and hybridization to 244k slide format 60-mer oligonucleotide microarrays for array-CGH (Agilent Mouse Genome CGH Microarray Kit 244A) were performed using genomic DNA from mouse HCCs as experimental samples and genomic DNA from the liver of a normal C57BL/6 mouse as a reference sample. The microarrays were scanned using a Micro Array Scanner, and data were extracted using Feature Extraction software and analyzed using CGH analytics 3.4 software according to the manufacturer's instructions (Agilent Technologies).

Gene expression profiling with microarrays. The ORF of human FEAT cDNA was subcloned into the pEF-DEST51 vector (Invitrogen, Life Technologies). NIH3T3 cells were transfected with pEF-DEST51-FEAT using HilyMax (Dojindo Laboratories). After 7 days of selection with 10 μg/ml blasticidin S (Kaken Pharmaceutical), colonies were picked and screened for clones in which FEAT protein was overexpressed. The *ccdB* gene in the pEF-DEST51 vector was deleted to construct the pEF-DEST51-ΔccdB plasmid, which was stably transfected into NIH3T3 cells to obtain control cell lines.

Total RNA was extracted from control (ΔccdB-1, -2, and -3) and FEAT-overexpressing NIH3T3 cell lines (FEAT-3, -15, and -20) using the RNeasy Mini kit (Qiagen). Gene expression profiling was performed with Sentrix Mouse WG-6 v2 BeadChip Array (Illumina) at the Research Support Center, Graduate School of Medical Sciences, Kyushu University. Raw gene expression data were first subjected to average normalization using BeadStudio 3.0 software. Average signals with detection *P*-values (based on Illumina replicate gene probes) > 0.01 were removed from analyses. GSEA was performed using the software available via the world wide web site (http://www.broadinstitute.org/gsea/).

Immunohistochemistry. Paraffin-embedded sections were deparaffinized with Clear-Advantage (Polysciences), rehydrated, treated with Citrate-based Antigen Unmasking Solution (Vector Laboratories), and stained using the ImmPRESS kit (Vector Laboratories) and ImmPACT Chromogen (Vector Laboratories) according to the manufacturer's instructions. The slides were counterstained with Mayer's Hematoxylin (Merck), and the coverslips were mounted with Gel/Mount aqueous mounting medium (Biomeda). The stained tissues were observed by the Zeiss Axioskop 2 *plus* microscope and images were acquired using the Zeiss AxioCam camera controlled by AxioVision software (Carl Zeiss MicroImaging). Images were also captured using the Leica MZ16 FA stereomicroscope, Leica DFC300 FX digital camera, and Leica IM500 Image Manager software (Leica Microsystems).

1. Bode, A. M. & Dong, Z. Cancer prevention research - then and now. *Nat. Rev. Cancer* **9**, 508–516 (2009).
2. Futreal, P. A. *et al.* A census of human cancer genes. *Nat. Rev. Cancer* **4**, 177–183 (2004).
3. Sjoblom, T. *et al.* The consensus coding sequences of human breast and colorectal cancers. *Science* **314**, 268–274 (2006).
4. Greenman, C. *et al.* Patterns of somatic mutation in human cancer genomes. *Nature* **446**, 153–158 (2007).
5. Wood, L. D. *et al.* The genomic landscapes of human breast and colorectal cancers. *Science* **318**, 1108–1113 (2007).

6. Jones, S. *et al.* Core signaling pathways in human pancreatic cancers revealed by global genomic analyses. *Science* **321**, 1801–1806 (2008).
7. Parsons, D. W. *et al.* An integrated genomic analysis of human glioblastoma multiforme. *Science* **321**, 1807–1812 (2008).
8. The Cancer Genome Atlas Research Network. Comprehensive genomic characterization defines human glioblastoma genes and core pathways. *Nature* **455**, 1061–1068 (2008).
9. Ding, L. *et al.* Somatic mutations affect key pathways in lung adenocarcinoma. *Nature* **455**, 1069–1075 (2008).
10. van der Brug, M. P. & Wahlestedt, C. Navigating genomic maps of cancer cells. *Nat. Biotechnol.* **28**, 241–242 (2010).
11. Meyerson, M., Gabriel, S. & Getz, G. Advances in understanding cancer genomes through second-generation sequencing. *Nat. Rev. Genet.* **11**, 685–696 (2010).
12. Stephens, P. J. *et al.* Complex landscapes of somatic rearrangement in human breast cancer genomes. *Nature* **462**, 1005–1010 (2009).
13. Stratton, M. R., Campbell, P. J. & Futreal, P. A. The cancer genome. *Nature* **458**, 719–724 (2009).
14. Hanahan, D. & Weinberg, R. A. Hallmarks of cancer: the next generation. *Cell* **144**, 646–674 (2011).
15. Vogelstein, B. & Kinzler, K. W. Cancer genes and the pathways they control. *Nat. Med.* **10**, 789–799 (2004).
16. Vander Heiden, M. G., Cantley, L. C. & Thompson, C. B. Understanding the Warburg effect: the metabolic requirements of cell proliferation. *Science* **324**, 1029–1033 (2009).
17. Shamji, A. F., Nghiem, P. & Schreiber, S. L. Integration of growth factor and nutrient signaling: implications for cancer biology. *Mol. Cell* **12**, 271–280 (2003).
18. Luo, J., Solimini, N. L. & Elledge, S. J. Principles of cancer therapy: oncogene and non-oncogene addiction. *Cell* **136**, 823–837 (2009).
19. Hanahan, D., Wagner, E. F. & Palmiter, R. D. The origins of oncomice: a history of the first transgenic mice genetically engineered to develop cancer. *Genes Dev.* **21**, 2258–2270 (2007).
20. Santarius, T., Shipley, J., Brewer, D., Stratton, M. R. & Cooper, C. S. A census of amplified and overexpressed human cancer genes. *Nat. Rev. Cancer* **10**, 59–64 (2010).
21. Lazebnik, Y. A., Cole, S., Cooke, C. A., Nelson, W. G. & Earnshaw, W. C. Nuclear events of apoptosis in vitro in cell-free mitotic extracts: a model system for analysis of the active phase of apoptosis. *J. Cell Biol.* **123**, 7–22 (1993).
22. Takahashi, A. *et al.* Cleavage of lamin A by Mch2 alpha but not CPP32: multiple interleukin 1 beta-converting enzyme-related proteases with distinct substrate recognition properties are active in apoptosis. *Proc. Natl. Acad. Sci. USA* **93**, 8395–8400 (1996).
23. Lai, C. H., Chou, C. Y., Ch'ang, L. Y., Liu, C. S. & Lin, W. Identification of novel human genes evolutionarily conserved in *Caenorhabditis elegans* by comparative proteomics. *Genome Res.* **10**, 703–713 (2000).
24. Kagan, R. M. & Clarke, S. Widespread occurrence of three sequence motifs in diverse S-adenosylmethionine-dependent methyltransferases suggests a common structure for these enzymes. *Arch. Biochem. Biophys.* **310**, 417–427 (1994).
25. Wirsing, L., Naumann, K. & Vogt, T. Arabidopsis methyltransferase fingerprints by affinity-based protein profiling. *Anal. Biochem.* **408**, 220–225 (2011).
26. Janicke, R. U., Sprengart, M. L., Wati, M. R. & Porter, A. G. Caspase-3 is required for DNA fragmentation and morphological changes associated with apoptosis. *J. Biol. Chem.* **273**, 9357–9360 (1998).
27. Kurokawa, M. & Kornbluth, S. Caspases and kinases in a death grip. *Cell* **138**, 838–854 (2009).
28. Schwarze, S. R., Hruska, K. A. & Dowdy, S. F. Protein transduction: unrestricted delivery into all cells? *Trends Cell Biol.* **10**, 290–295 (2000).
29. Velculescu, V. E. *et al.* Analysis of human transcriptomes. *Nat. Genet.* **23**, 387–388 (1999).
30. Naugler, W. E. *et al.* Gender disparity in liver cancer due to sex differences in MyD88-dependent IL-6 production. *Science* **317**, 121–124 (2007).
31. Anisimov, V. N., Ukraintseva, S. V. & Yashin, A. I. Cancer in rodents: does it tell us about cancer in humans? *Nat. Rev. Cancer* **5**, 807–819 (2005).
32. Frese, K. K. & Tuveson, D. A. Maximizing mouse cancer models. *Nat. Rev. Cancer* **7**, 645–658 (2007).
33. Grivennikov, S. I., Greten, F. R. & Karin, M. Immunity, inflammation, and cancer. *Cell* **140**, 883–899 (2010).
34. Hussain, S. P., Schwank, J., Staib, F., Wang, X. W. & Harris, C. C. TP53 mutations and hepatocellular carcinoma: insights into the etiology and pathogenesis of liver cancer. *Oncogene* **26**, 2166–2176 (2007).
35. Toledo, F. & Wahl, G. M. Regulating the p53 pathway: in vitro hypotheses, in vivo veritas. *Nat. Rev. Cancer* **6**, 909–923 (2006).
36. Laurent-Puig, P. & Zucman-Rossi, J. Genetics of hepatocellular tumors. *Oncogene* **25**, 3778–3786 (2006).
37. Zender, L. *et al.* Identification and validation of oncogenes in liver cancer using an integrative oncogenomic approach. *Cell* **125**, 1253–1267 (2006).
38. Latres, E. *et al.* Role of the F-box protein Skp2 in lymphomagenesis. *Proc. Natl. Acad. Sci. USA* **98**, 2515–2520 (2001).
39. Clancy, J. L. *et al.* EDD, the human orthologue of the hyperplastic discs tumour suppressor gene, is amplified and overexpressed in cancer. *Oncogene* **22**, 5070–5081 (2003).
40. Graham, M. & Adams, J. M. Chromosome 8 breakpoint far 3′ of the c-myc oncogene in a Burkitt's lymphoma 2;8 variant translocation is equivalent to the murine pvt-1 locus. *EMBO J.* **5**, 2845–2851 (1986).
41. Farazi, P. A. & DePinho, R. A. Hepatocellular carcinoma pathogenesis: from genes to environment. *Nat. Rev. Cancer* **6**, 674–687 (2006).
42. Chin, L. & Gray, J. W. Translating insights from the cancer genome into clinical practice. *Nature* **452**, 553–563 (2008).
43. Subramanian, A. *et al.* Gene set enrichment analysis: a knowledge-based approach for interpreting genome-wide expression profiles. *Proc. Natl. Acad. Sci. USA* **102**, 15545–15550 (2005).
44. Gschwind, A., Fischer, O. M. & Ullrich, A. The discovery of receptor tyrosine kinases: targets for cancer therapy. *Nat. Rev. Cancer* **4**, 361–370 (2004).
45. Rubin, L. L. & de Sauvage, F. J. Targeting the Hedgehog pathway in cancer. *Nat. Rev. Drug Discov.* **5**, 1026–1033 (2006).
46. Varjosalo, M. & Taipale, J. Hedgehog: functions and mechanisms. *Genes Dev.* **22**, 2454–2472 (2008).
47. Kim, B. *et al.* Expression profiling and subtype-specific expression of stomach cancer. *Cancer Res.* **63**, 8248–8255 (2003).
48. Gratias, S. *et al.* Genomic gains on chromosome 1q in retinoblastoma: consequences on gene expression and association with clinical manifestation. *Int. J. Cancer* **116**, 555–563 (2005).
49. Vincent-Salomon, A. *et al.* Integrated genomic and transcriptomic analysis of ductal carcinoma in situ of the breast. *Clin. Cancer Res.* **14**, 1956–1965 (2008).
50. Kim, J., Chu, J., Shen, X., Wang, J. & Orkin, S. H. An extended transcriptional network for pluripotency of embryonic stem cells. *Cell* **132**, 1049–1061 (2008).
51. Chen, X. *et al.* Integration of external signaling pathways with the core transcriptional network in embryonic stem cells. *Cell* **133**, 1106–1117 (2008).
52. Liu, X. *et al.* Yamanaka factors critically regulate the developmental signaling network in mouse embryonic stem cells. *Cell Res.* **18**, 1177–1189 (2008).
53. Kim, J. *et al.* A Myc network accounts for similarities between embryonic stem and cancer cell transcription programs. *Cell* **143**, 313–324 (2010).
54. Mahon, P. B. *et al.* Genome-wide linkage and follow-up association study of postpartum mood symptoms. *Am. J. Psychiatry* **166**, 1229–1237 (2009).
55. Mill, J. *et al.* Epigenomic profiling reveals DNA-methylation changes associated with major psychosis. *Am. J. Hum. Genet.* **82**, 696–711 (2008).
56. Rebouissou, S. *et al.* Frequent in-frame somatic deletions activate gp130 in inflammatory hepatocellular tumours. *Nature* **457**, 200–204 (2009).
57. Thorgeirsson, S. S. & Grisham, J. W. Molecular pathogenesis of human hepatocellular carcinoma. *Nat. Genet.* **31**, 339–346 (2002).
58. Kufe, D. W. Mucins in cancer: function, prognosis and therapy. *Nat. Rev. Cancer* **9**, 874–885 (2009).
59. Altieri, D. C. Survivin, cancer networks and pathway-directed drug discovery. *Nat. Rev. Cancer* **8**, 61–70 (2008).
60. Ho, A., Schwarze, S. R., Mermelstein, S. J., Waksman, G. & Dowdy, S. F. Synthetic protein transduction domains: enhanced transduction potential in vitro and in vivo. *Cancer Res.* **61**, 474–477 (2001).

Acknowledgements

We thank T. Honjo, I. Chung-Okazaki, A. Shirahata, T. Hashimoto, C. F. Clarke, P. Gin, W. Frommer, X. Wang, F. Toyoshima-Morimoto, and A. K. Munirajan for reagents; H. Ohno for cell lines; M. Sugimoto, K. Igarashi, and the Research Support Center, Graduate School of Medical Sciences, Kyushu University for technical support; S. H. Kaufmann, T. Marumoto, and A. Suzuki for critically reading; K. Sakurai, Y. Nakamura, N. Shibano-Kondo, A. Kitabayashi-Akao, S. Ito, and M. Okada for technical assistance; T. Moriguchi, M. Taketo, T. Hori, T. Ichinohe, K. Yamamoto, M. Sasada, T. Uchiyama, A. Uemura, A. Kotani-Yoshida, T. Ozaki, H. Kageyama, S. Haraguchi, M. Mizoe-Amako, T. Nakamura, and E. Nishida for discussions and suggestions; J. Hirai, Y. Asano-Ashida, K. Miyata, M. Ushijima, and K. Maekawa for secretarial assistance. This work was supported by Grants-in-Aid from the Ministry of Education, Culture, Sports, Science, and Technology of Japan, the Academic Research Grant from Kyoto University, and a grant from the Tokyo Biochemical Research Foundation.

Author contributions

AT designed the project. AT, DT, AN, and KTani designed experiments. AT, HT, KTakahashi, TT, KM, AI, OK, and KY performed a significant amount of the experimental work. AT, MO, and TK performed most of the data collection and data analysis. AT wrote the main manuscript text and prepared figures and tables. All authors reviewed the manuscript.

Additional information

Supplementary Information accompanies this paper at http://www.nature.com/scientificreports

Author Information Human FEAT cDNAs are deposited in GenBank (AB242174 and AB242175). Microarray data are deposited in GEO (expression microarray, GSE18299; array-CGH, GSE18403).

Competing financial interests: The authors declare no competing financial interests.

How to cite this article: Takahashi, A. *et al.* A novel potent tumour promoter aberrantly overexpressed in most human cancers. *Sci. Rep.* **1**, 15; DOI:10.1038/srep00015 (2011).

SCIENTIFIC REPORTS

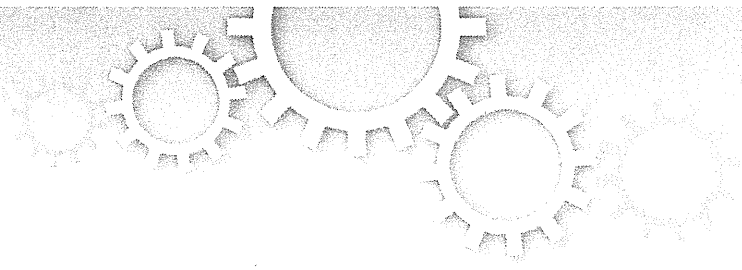

DOI: 10.1038/srep00049

SUBJECT AREAS:
ONCOGENESIS
CANCER MODELS
CELL DEATH
CANCER

SCIENTIFIC REPORTS:
1 : 15
DOI: 10.1038/srep00015
(2011)

Published:
14 June 2011

Updated:
23 January 2013

CORRIGENDUM: A novel potent tumour promoter aberrantly overexpressed in most human cancers

Atsushi Takahashi, Hisashi Tokita, Kenzo Takahashi, Tomoharu Takeoka, Kosho Murayama, Daihachiro Tomotsune, Miki Ohira, Akihiro Iwamatsu, Kazuaki Ohara, Kazufumi Yazaki, Tadayuki Koda, Akira Nakagawara & Kenzaburo Tani

Since the publication of this paper, the authors have discovered an error in the Results section of the paper, which they would like to correct.

The statement "In particular, HCCs caused by aflatoxin characteristically have the S376A mutation in p53" should read "In particular, HCCs caused by aflatoxin characteristically have the R249S mutation in p53".

OPEN ACCESS Freely available online

PLoS one

Oncogenic LMO3 Collaborates with HEN2 to Enhance Neuroblastoma Cell Growth through Transactivation of *Mash1*

Eriko Isogai[1,2], Miki Ohira[2], Toshinori Ozaki[3], Shigeyuki Oba[4], Yohko Nakamura[1], Akira Nakagawara[1]*

1 Division of Biochemistry and Innovative Cancer Therapeutics, Chiba Cancer Center Research Institute, Chuoh-ku, Chiba, Japan, **2** Laboratory of Cancer Genomics, Chiba Cancer Center Research Institute, Chuoh-ku, Chiba, Japan, **3** Laboratory of Anti-Tumor Research, Chiba Cancer Center Research Institute, Chuoh-ku, Chiba, Japan, **4** Integrated Systems Biology Laboratory, Department of Systems Science, Graduate School of Informatics, Kyoto University, Gokasho, Uji, Kyoto, Japan

Abstract

Expression of *Mash1* is dysregulated in human neuroblastoma. We have also reported that LMO3 (LIM-only protein 3) has an oncogenic potential in collaboration with neuronal transcription factor HEN2 in neuroblastoma. However, the precise molecular mechanisms of its transcriptional regulation remain elusive. Here we found that LMO3 forms a complex with HEN2 and acts as an upstream mediator for transcription of *Mash1* in neuroblastoma. The high levels of *LMO3* or *Mash1* mRNA expression were significantly associated with poor prognosis in 100 primary neuroblastomas. The up-regulation of *Mash1* remarkably accelerated the proliferation of SH-SY5Y neuroblastoma cells, while siRNA-mediated knockdown of *LMO3* induced inhibition of growth of SH-SY5Y cells in association with a significant down-regulation of *Mash1*. Additionally, overexpression of both LMO3 and HEN2 induced expression of *Mash1*, suggesting that they might function as a transcriptional activator for *Mash1*. Luciferase reporter assay demonstrated that the co-expression of LMO3 and HEN2 attenuates HES1 (a negative regulator for *Mash1*)-dependent reduction of luciferase activity driven by the *Mash1* promoter. Chromatin immunoprecipitation assay revealed that LMO3 and HEN2 reduce the amount of HES1 recruited onto putative HES1-binding sites and E-box within the *Mash1* promoter. Furthermore, both LMO3 and HEN2 are physically associated with HES1 by immunoprecipitation assay. Thus, our present results suggest that a transcriptional complex of LMO3 and HEN2 may contribute to the genesis and malignant phenotype of neuroblastoma by inhibiting HES1 which suppresses the transactivation of *Mash1*.

Citation: Isogai E, Ohira M, Ozaki T, Oba S, Nakamura Y, et al. (2011) Oncogenic LMO3 Collaborates with HEN2 to Enhance Neuroblastoma Cell Growth through Transactivation of *Mash1*. PLoS ONE 6(5): e19297. doi:10.1371/journal.pone.0019297

Editor: Laszlo Tora, Institute of Genetics and Molecular and Cellular Biology, France

Received December 21, 2010; **Accepted** March 31, 2011; **Published** May 5, 2011

Funding: This work was supported in part by a Grant-in-Aid from the Ministry of Health, Labour and Welfare for the Third Term Comprehensive Control Research for Cancer; a Grant-in-Aid for Scientific Research on Priority Areas from the Ministry of Education, Culture, Sports, Science and Technology, Japan; and a Grant-in-Aid for Scientific Research from Japan Society for the Promotion of Science. The funders had no role in study design, data collection and analysis, decision to publish, or preparation of the manuscript.

Competing Interests: The authors have declared that no competing interests exist.

* E-mail: akiranak@chiba-cc.jp

Introduction

Neuroblastoma is one of the typical childhood cancers and is originated from sympathetic cell lineage of the neural crest [1,2]. Since the tumor never occurs from the other lineages of the neural crest, the oncogenic events to cause neuroblastoma might be strictly regulated in a lineage-specific manner [1,2].

LIM-only protein (LMO) family is composed of four members, LMO1, LMO2, LMO3 and LMO4. Although LMO proteins lack a DNA-binding activity, accumulating evidence suggest that LMO proteins are involved in transcriptional regulation of specific target genes in collaboration with other transcription factors [3]. Genetic analyses demonstrated that LMO1 and LMO2 contribute to the genesis of immature and aggressive T-cell leukemia [4], whereas LMO4 was implicated in development of breast cancer [5,6]. Previously, we reported that *LMO3* is expressed at significantly high levels in human unfavorable neuroblastomas relative to favorable ones, and has an oncogenic potential in neuroblastoma [7]. LMO3 formed a complex with neuronal-specific basic helix-loop-helix (bHLH) transcription factor HEN2, which was also expressed at higher levels in unfavorable neuroblastoma than favorable one, raising a possibility that LMO3 may form a complex with HEN2 and play an important role in genesis and development of neuroblastoma through transcriptional regulation of as yet unidentified target gene(s).

A proneural bHLH transcription factor termed Mash1 plays a critical role in development of sympathetic neuron and is highly expressed in neuroblastoma [8,9]. However, its possible contribution to development of neuroblastoma remains elusive. A bHLH protein termed HES1 acts as a negative regulator for *Mash1* [10]. Intriguingly, studies in *Drosophila* demonstrated that expression levels of *achaete-scute*, a *Drosophila* homolog of *Mash1*, are remarkably induced by a transcriptional complex composed of *Drosophila* homolog of LMO (dLMO) and bHLH proteins [11,12].

In this study, we examined whether there could exist functional relationship between LMO3/HEN2 and Mash1 in neuroblastoma, and found that LMO3/HEN2 attenuates HES1 function and enhances transactivation of *Mash1*, leading to aggressive phenotype of neuroblastoma.

Results

High levels of *Mash1* expression is associated with poor outcome of neuroblastoma

Mash1 is constitutively expressed at high levels in neuroblastoma cell lines and primary neuroblastoma tumors [9,13], however, its prognostic significance remained elusive. On the other hand, expression of *LMO3* was significantly associated with poor outcome of the patients [7]. To verify whether a significant relationship could be observed between expression of *LMO3* and that of *Mash1* in primary neuroblastomas, we quantitatively measured the expression levels of *LMO3* and *Mash1* mRNA in 100 primary tumors by using a quantitative real-time RT-PCR. The student's t-test showed that high expression of *LMO3* was significantly associated with ≥1 year of age ($p = 0.036$), low expression of *TrkA* ($p = 0.003$) and *MYCN* amplification ($p = 0.04$), but not with the tumor stage ($p = 0.17$), tumor origin ($p = 0.083$) and Shimada classification ($p = 0.082$). High expression of *Mash1* was significantly associated with advanced tumor stage ($p = 0.004$) but not with age ($p = 0.81$), *TrkA* expression ($p = 0.4$), *MYCN* copy number ($p = 0.11$), tumor origin ($p = 0.2$) and Shimada classification ($p = 0.45$) (Table S1). No significant relationship was observed between *LMO3* and *Mash1* mRNA expression levels (the Pearson correlation coefficient was 0.27). Kaplan-Meier survival curves indicated that high expression of *LMO3* as well as that of *Mash1* were significantly associated with poor prognosis (log-rank test, $p = 0.006$ and $p = 0.037$, respectively; Figure 1). The univariate analysis according to the Cox proportional hazard model also indicated that the expression levels of *Mash1* and those of *LMO3* were significantly associated with poor outcome of the patients ($p = 0.048$ and $p = 0.012$, respectively; Table S2). The multivariate Cox proportional hazard model analysis showed that the expression of *Mash1* was significantly independent prognostic factor from *LMO3* expression and age, marginally from *MYCN* copy number and origin, but not from the disease stage, and that the expression of *LMO3* was significantly independent prognostic factor from *Mash1* expression, age, the disease stage and origin, but not from *MYCN* copy number (Table S2). Thus, the results obtained from the primary neuroblastomas suggested that both high mRNA expression of *LMO3* and *Mash1* were strongly associated with poor prognoses of the patients with neuroblastoma but the way of contribution of those seemed to be rather independent.

Mash1 mediates growth promotion of neuroblastoma cells

Since *Mash1* is highly expressed in primary neuroblastoma [9] and its higher expression was significantly correlated with poor prognosis of the patient with neuroblastoma, we then investigated a possible contribution of Mash1 to neuroblastoma cell growth. For this purpose, we established three stable *Mash1* infectants derived from the parental SH-SY5Y neuroblastoma cells expressing exogenous Mash1 (M-1, M-2 and M-3) and two control vector alone infectants (V-1 and V-2) by retrovirus-mediated gene transfer (Figure 2A). As shown in Figure 2B, constitutive expression of *Mash1* in SH-SY5Y cells resulted in a remarkable increase in their growth rate as compared with the control infectants, suggesting that Mash1 is involved in regulation of neuroblastoma cell growth.

As described previously [7], LMO3 has an oncogenic potential in collaboration with HEN2 in neuroblastoma cells. We then asked whether or not LMO3 is involved in the Mash1-mediated enhancement of cell growth. As shown in Figure 2C, siRNA-mediated knockdown of *LMO3* in SH-SY5Y cells was significantly associated with a down-regulation of *Mash1*. Additionally, LMO3-knocked down SH-SY5Y cells showed a slower growth rate than the control SH-SY5Y cells (Figure 2D), which might be at least in part due to reduction of *Mash1*. We conducted the same experiments by using another cell line SK-N-BE and obtained the similar results (Figure S1A and B). We then hypothesized that *Mash1* could be one of transcriptional targets of LMO3/HEN2 complex.

LMO3/HEN2 mediate transcriptional induction of *Mash1*

To address whether *Mash1* transcription could be induced by LMO3/HEN2, SH-SY5Y cells were infected with the indicated combinations of recombinant adenoviruses encoding HA-LMO3 or FLAG-HEN2, and the expression levels of *Mash1* were examined by semi-quantitative RT-PCR. Time course experiments demonstrated that *Mash1* is readily detectable in cells expressing HA-LMO3 alone or in cells co-expressing with HA-LMO3 and FLAG-HEN2 at 48 h after infection

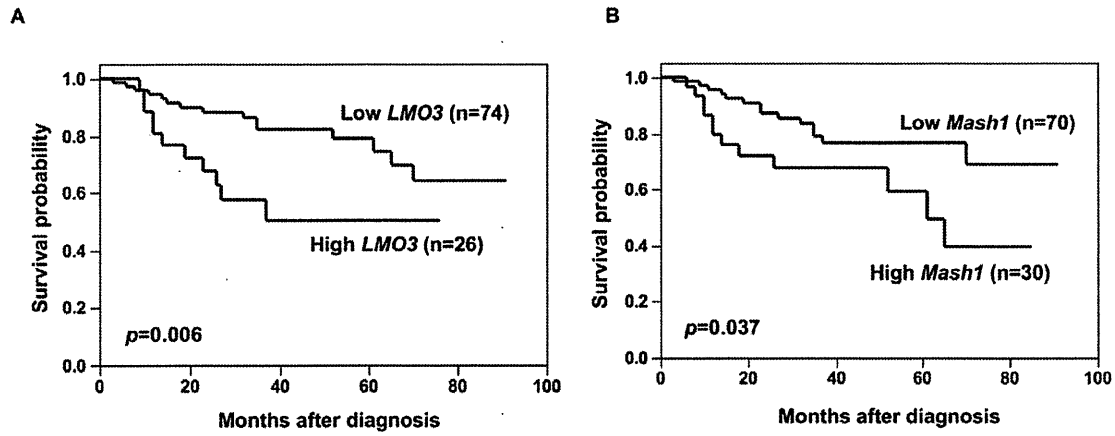

Figure 1. Kaplan-Meier survival curves of patients with neuroblastomas based on high or low expression of *LMO3* (A) or *Mash1* (B). Kaplan-Meier survival curves (n = 100) in relation to the expression levels of *LMO3* or *Mash1* (average cutoff). The patients with high expression of *LMO3* or *Mash1* represented significantly poor prognosis than those with its low expression.
doi:10.1371/journal.pone.0019297.g001

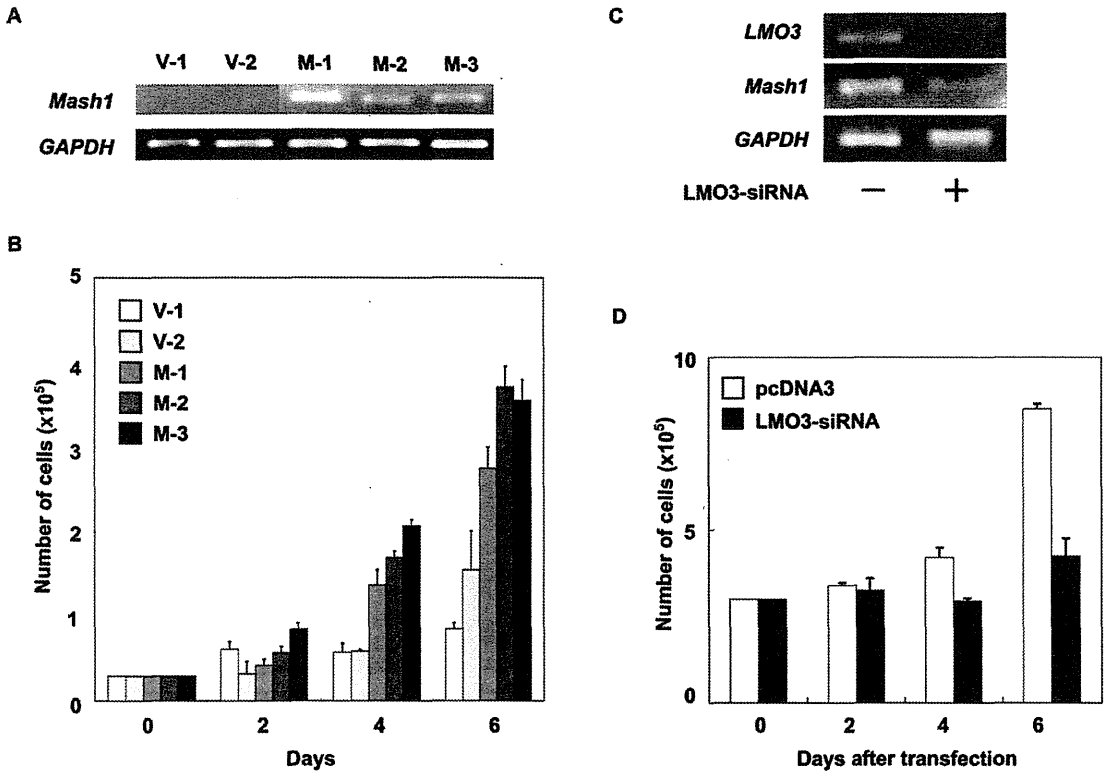

Figure 2. Mash1-mediated growth promotion of neuroblastoma cells. (A) Enforced expression of *Mash1*. Neuroblastoma SH-SY5Y cells were infected with empty retrovirus or with retrovirus encoding Mash1 and established two control infectants (V-1 and V-2) and three infectants expressing *Mash1* (M-1, M-2 and M-3). Total RNA was extracted from the indicated cell clones and subjected to RT-PCR to examine expression levels of *Mash1*. *GAPDH* was used as an internal control. (B) Mash1-mediated growth promotion. The indicated infectants were seeded at a density of 3×10^4/cell culture dish and allowed to attach overnight. At the indicated time periods, number of viable cells was measured. (C) siRNA-mediated knockdown of LMO3. SH-SY5Y cells were transfected with empty plasmid (4 μg) or with expression plasmid for siRNA targeting LMO3 (4 μg). Forty-eight hours after transfection, total RNA was prepared and analyzed for expression levels of *LMO3* and *Mash1* by RT-PCR. (D) Decreased growth rate in LMO3-knocked down cells. SH-SY5Y cells (3×10^5 cells/cell culture dish) were transfected as in (C). Forty-eight hours after transfection, cells were transferred into fresh medium. At the indicated time points, number of viable cells was measured.
doi:10.1371/journal.pone.0019297.g002

(Figure 3A). Seventy-two hours after infection, co-expression of HA-LMO3 and FLAG-HEN2 led to a significant induction of *Mash1*. The induction of *Mash1* was also observed in SK-N-BE cells transfected with expression vector HA-LMO3 alone or HA-LMO3 and FLAG-HEN2 at 72 h after transfection (Figure S1C). To further confirm these observations, we generated a luciferase reporter construct carrying human *Mash1* promoter (pluc-Mash1). As shown in Figure 3B, the 5′-upstream region of *Mash1* gene contains three putative HES1-binding sites and one E-box. In both SH-SY5Y cells and SK-N-BE cells, siRNA-mediated knockdown of human *LMO3* reduced promoter activity of *Mash1* in a dose-dependent manner (Figure 3C and Figure S1D). For luciferase reporter assay without siRNA for human LMO3, we used mouse neuroblastoma Neuro2a cells which displayed higher transfection efficiency than human neuroblastoma cells as examined by GFP staining (data not shown). Consistent with the above expression studies, LMO3 enhanced luciferase activity driven by *Mash1* promoter (Figure 3D). Furthermore, we examined the effect of HEN2 on *Mash1* promoter activity in Neuro2a cells, showing that HEN2 itself inhibited *Mash1* promoter activity (Figure 3E). Intriguingly, however, LMO3 interfered with HEN2 function, resulting in up-regulation of *Mash1* transcription (Figure 3F). Thus, it is likely that the LMO3 complex including HEN2 and HES1 regulates transcription of *Mash1*. The mRNA expression pattern of *LMO3*, *HEN2*, *Mash1* and *HES1*, a negative regulator of *Mash1* transcription, in neuroblastoma cell lines is shown in Figure S2.

LMO3/HEN2 attenuates HES1-dependent down-regulation of *Mash1*

As reported previously [10], HES1 is one of the negative regulators for *Mash1*. In accordance with the previous observations, enforced expression of HES1 dramatically reduced luciferase activity driven by *Mash1* promoter (Figure 4A). The inhibitory effect of HES1 on *Mash1* promoter was stronger than that of HEN2. To investigate the relationships between HES1 and LMO3/HEN2 in transcriptional regulation of *Mash1*, we examined effects of HEN2 and LMO3 on HES1-dependent down-regulation of *Mash1* (Figure 4B). The HES1-dependent inhibition of *Mash1* promoter activity was attenuated by co-expression with FLAG-HEN2 alone or with co-expression with FLAG-HEN2 plus HA-LMO3. Inhibitory effects of FLAG-HEN2 plus HA-LMO3 on HES1 were larger than that of FLAG-HEN2 alone, suggesting that LMO3/HEN2 complex plays a critical role in regulation of *Mash1* transcription by neutralizing the inhibitory effect of HES1.